

# The development of a bioengineered organ germ method

Kazuhisa Nakao<sup>1,2</sup>, Ritsuko Morita<sup>1,2</sup>,  
Yasumitsu Saji<sup>1,2</sup>, Kentaro Ishida<sup>1,2</sup>,  
Yusuke Tomita<sup>1,2</sup>, Miho Ogawa<sup>1,2</sup>, Masahiro Saitoh<sup>3</sup>,  
Yasuhiro Tomooka<sup>1,2</sup> & Takashi Tsuji<sup>1,2</sup>

**To bioengineer ectodermal organs such as teeth and whisker follicles, we developed a three-dimensional organ-germ culture method. The bioengineered tooth germ generated a structurally correct tooth, after both *in vitro* organ culture as well as transplantation under a tooth cavity *in vivo*, showing penetration of blood vessels and nerve fibers. Our method provides a substantial advance in the development of bioengineered organ replacement strategies and regenerative therapies.**

The approaches that have been adopted in regenerative medicine are influenced by our understanding of embryonic development, stem-cell biology and tissue-engineering technology<sup>1–3</sup>. To restore the partial loss of organ function, stem cell transplantation therapies have been developed<sup>1–3</sup>. The ultimate goal of regenerative therapy, however, is to develop fully functioning bioengineered organs that can replace lost or damaged organs after disease, injury or aging<sup>1–3</sup>. Almost all organs arise from the organ germ, which is induced by the reciprocal interactions between the epithelium and mesenchyme in the developing embryo<sup>4–7</sup>. Therefore, it has been suggested that to properly reproduce the developmental process of organogenesis, it will be necessary to fully reconstitute these events in an artificially bioengineered organ<sup>7</sup>.

The purpose of our study was to improve bioengineering methods for three-dimensional organ germs using completely dissociated epithelial and mesenchymal cells. For this purpose, we adopted the tooth and whisker follicle germs as model ectodermal organs. Although previous studies have demonstrated three-dimensional reconstruction of an artificial organ germ from dissociated single cells *in vitro*, improvement in bioengineering technology is needed before reconstitution of a primordial organ precisely replicates tooth organogenesis as observed in embryonic development<sup>7–11</sup>. The first step in multicellular aggregation of epithelial and mesenchymal cells is multicellular assembly by self-reorganization in each cell type through cell movement and selective cell adhesion until the cells reach an equilibrium

configuration<sup>12</sup>. Next the reciprocal interactions between epithelial and mesenchymal cell layers initiate organogenesis and regulate differentiation and morphogenesis<sup>5,6</sup>. The cell potential for self-reorganization and tissue reconstitution, however, is different among cell types of various organs<sup>10</sup>. Here we describe a bioengineered organ germ method with cell compartmentalization *in vitro*, which is applicable to not only *in vitro* organ culture but also *in vivo* transplantation. Our model improves our understanding of the principles by which organ reconstitution can be achieved with tissues that have been bioengineered *in vitro* and increases the potential for the use of bioengineered organ replacement in future regenerative therapies.

We first investigated the possibility of developing a bioengineered tooth germ using completely dissociated single cells from epithelial and mesenchymal tissues of incisor tooth germ at cap stage from the lower jaw in ED14.5 mice (Fig. 1a, Supplementary Methods online and Supplementary Fig. 1 online). The explants reconstituted by epithelial or mesenchymal cells alone generated keratinized oral epithelium-like structures or bone, respectively, but not a complete tooth (Supplementary Fig. 1). The explants that reconstituted the cell compartmentalization between epithelial and mesenchymal cells at a low-cell density ( $0.5\text{--}1 \times 10^8$  cells/ml) or that did not form cell compartmentalization at high-cell density ( $5 \times 10^8$  cells/ml), also could not generate a correct tooth structure (Supplementary Fig. 1). To reconstitute a bioengineered tooth germ with the correct cell compartmentalization between epithelium- and mesenchyme-derived single cells, we injected the cells in turn at high cell density ( $5 \times 10^8$  cells/ml) into adjacent regions within a collagen gel drop (Fig. 1a and Supplementary Methods). Within 1 d of organ culture, we observed formation of a tooth germ with the appropriate compartmentalization between epithelial and mesenchymal cells and cell-to-cell compaction (Fig. 1b). We then performed transplantations of this bioengineered tooth germ into subrenal capsules in mice and over a 10-d period observed by histology that this primordium could generate plural incisors, in which tissue elements such as odontoblasts, dentin, dentinal tubules, ameloblasts, enamel, Tomes' process, dental pulp, root, blood vessels, alveolar bone and periodontal ligaments, were arranged appropriately when compared with a natural tooth (Fig. 1c, Supplementary Fig. 1 and Supplementary Fig. 2 online). We also found that this occurred with a frequency of 100% in 50 separate transplants. *In situ* hybridization analysis of the reconstituted teeth showed mRNA for dentin sialoprotein, amelogenin and periostin, specific markers for odontoblasts, ameloblasts and periodontal ligaments, respectively (Supplementary Fig. 1). We next examined the origin of the cell types derived from epithelium or mesenchyme using bioengineered tooth germ from GFP-transgenic mice. GFP-transgenic mouse-derived mesenchymal cells generated

<sup>1</sup>Department of Biological Science and Technology, Faculty of Industrial Science and Technology, Tokyo University of Science, Noda, Chiba, 278-8510, Japan.

<sup>2</sup>Tissue Engineering Research Center, Tokyo University of Science, Noda, Chiba, 278-8510, Japan. <sup>3</sup>Department of Molecular and Cellular Biochemistry, Osaka University Graduate School of Dentistry, Osaka, Japan. Correspondence should be addressed to T.T. (t-tsuji@rs.noda.tus.ac.jp).

RECEIVED 23 OCTOBER 2006; ACCEPTED 9 JANUARY 2007; PUBLISHED ONLINE 18 FEBRUARY 2007; DOI:10.1038/NMETH1012



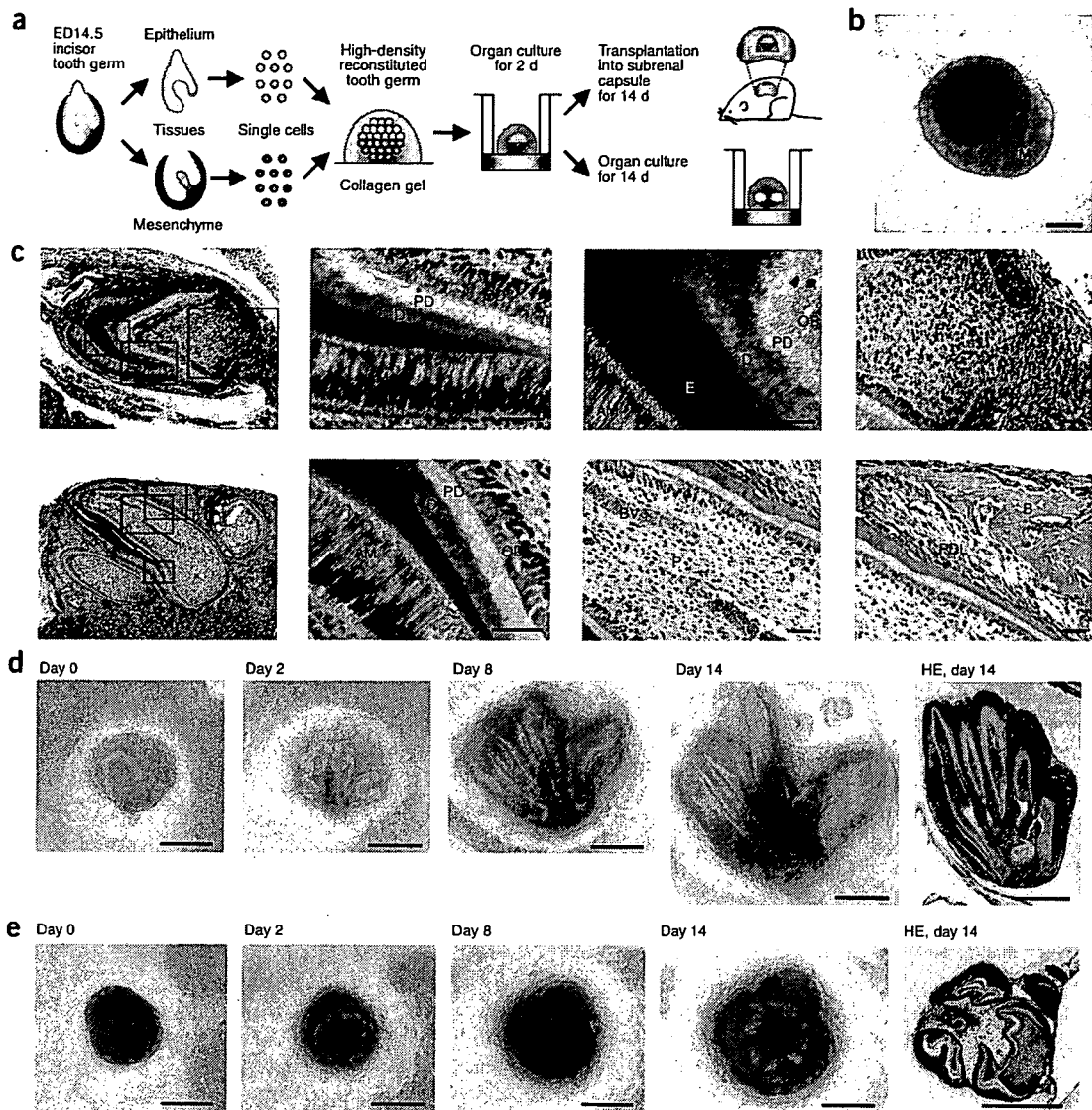


**Figure 1** | Generation of a whole tooth using bioengineered tooth germ derived from dissociated single cells *in vivo*. (a) Schematic of the bioengineering technology used for the generation of a reconstituted tooth germ. The epithelial and mesenchymal tissues isolated from incisor tooth germ of ED14.5 mice were completely dissociated into single cells. The bioengineered incisor tooth germ was then reconstituted using these dissociated cells that showed cell compartmentalization at a high cell density. The explants were either transplanted beneath a subrenal capsule or were continuously cultured. (b) Phase-contrast image of bioengineered incisor tooth germ after 1 d of cultivation. E, epithelial cells; M, mesenchymal cells. Scale bar, 250  $\mu\text{m}$ . (c) Histological analysis of the reorganized tooth germ under a subrenal capsule for 10 d (top) and 14 d (bottom) after transplantation. AM, ameloblasts; B, alveolar bone; BV, blood vessels; PD, pre-dentin; D, dentin; E, enamel; OD, odontoblasts; P, pulp cells; PDL, periodontal ligaments. Scale bars, 50  $\mu\text{m}$ . (d,e) Time course images of a bioengineered incisor and molar tooth germ in an *in vitro* organ culture. Bioengineered incisor (d) and molar (e) tooth germ were reconstituted between dissociated epithelial and mesenchymal cells isolated from each incisor and molar tooth germ of ED14.5 mice, respectively. Multiple induction of primordia can be observed by phase contrast microscopy (IX70 Olympus). Bioengineered incisor and molar that had been cultured for 14 d were also analyzed by hematoxylin-eosin staining (HE). Scale bars, 500  $\mu\text{m}$ .

not only odontoblasts and dental pulp derived from dental papilla, but also alveolar bone and periodontal ligaments, which are derived from dental follicles (Supplementary Fig. 1). GFP-transgenic mouse-derived epithelial cells generated ameloblasts (Supplementary Fig. 1). We also determined that bioengineered tooth germ reconstituted with epithelial and mesenchymal cells isolated from incisor tooth germ at bell stage in ED16.5 mice could not develop into teeth (data not shown). This result indicates that the

developmental stage of the tooth germ is critical for the application of this method.

We next examined whether our bioengineered tooth germ had the capability of generating teeth via *in vitro* organ cultures (Supplementary Methods). Notably, our experiments indicate that bioengineered tooth germ successfully develops teeth *in vitro*, and that these structures have correctly placed mineralized tissue and cell types (Fig. 1d,e and Supplementary Fig. 2). Using

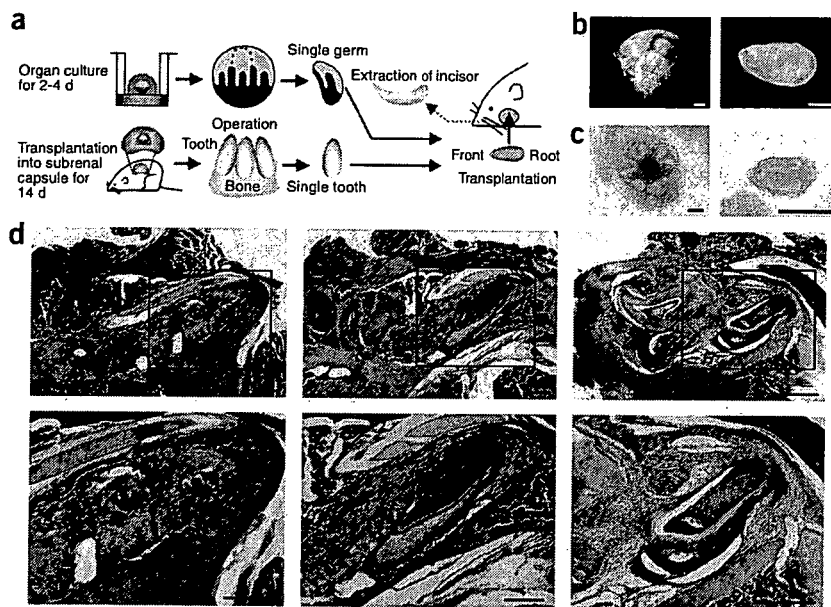


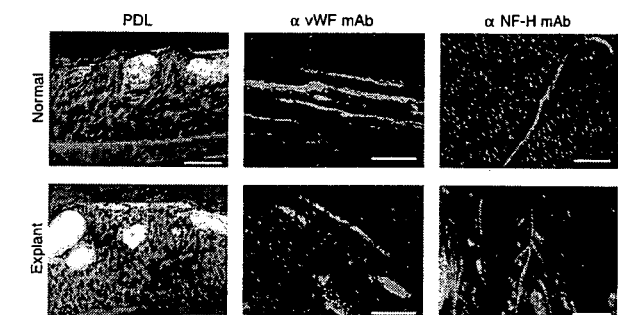
**Figure 2** | Development of the bioengineered incisor in the tooth cavity of adult mice. (a) Schematic representation of the transplantation procedure. A bioengineered incisor developed under a subrenal capsule and reconstituted incisor tooth germ cultured for 2 d were each separated surgically into single primordia. These explants were then transplanted into a tooth cavity generated by the extraction of a mandibular incisor from the vestibular surface of an adult mouse. (b) Representative phase contrast images showing a bioengineered incisor developed in a subrenal capsule environment for 14 days (left) and a tooth separated from reconstituted tissue in the subrenal capsule and used for transplantation (right). Scale bars, 500  $\mu\text{m}$ . (c) Separation of individual primordia (dotted circle) from bioengineered tooth germ that had been cultured for 2 d. Scale bars, 250  $\mu\text{m}$ . (d) Histological analysis of the explants at 14 d after transplantation into a tooth cavity. Images from the control experiment (left) and transplants isolated from a single incisor primordium (center) and a single tooth developed in the subrenal capsule (right) are shown. Boxes indicate the area shown at a higher magnification in the lower panels. Scale bars, 1 mm.

time-course images, we observed that both incisor and molar-derived bioengineered tooth germ reconstituted using dissociated epithelial and mesenchymal cells from the tooth germ of an incisor or a molar, respectively, gave rise to multiple primordia from the periphery of the boundary surface between epithelial and mesenchymal cells after 2–3 d of growth. Thereafter we observed development of plural teeth containing natural tooth materials and correct cell placement from each primordium (Fig. 1d,e). Notably, in the tooth germ cultures, the epithelial cells invaginated and multiplied prominently in the mesenchymal aggregates, in combination with cells isolated from normal and GFP-transgenic mice (Supplementary Fig. 1). Furthermore, the development of chimeric bioengineered tooth germs, prepared with epithelial and mesenchymal cells of normal and GFP-transgenic mice in

**Figure 3** | Analysis of periodontal ligaments, endothelial cells of tooth blood vessels and neural filaments in a bioengineered tooth. Incisors isolated from 3 day-post-birth normal mice (normal; top) and a bioengineered tooth (explant; bottom) are shown. Periodontal ligaments (PDL) were morphologically analyzed by haematoxylin-eosin staining (left), and the endothelial cells of blood vessels ( $\alpha$ vWF mAb; center) and neurons (NF-H mAb; right) were analyzed by immunoreactivity with specific antibodies for von Willebrand factor (vWF) and neurofilament-H (NF-H), respectively. Fluorescence and differential interference contrast (DIC) images were merged. Scale bar, 50  $\mu\text{m}$ .

various conditions, clearly demonstrated that the chimeric primordia were reconstituted by completely dissociated single cells (Supplementary Fig. 1 and Supplementary Note online). Direct cell-to-cell communication induced by high cell density and cell compartmentalization is essential in tooth organogenesis<sup>13</sup> and possibly that of other organs. Beta-1 integrin, CD29, is expressed at the boundary surface between epithelial and mesenchymal cells<sup>14</sup>. Treatment of dissociated epithelial and mesenchymal cells by neutralizing CD29 monoclonal antibodies inhibited tooth formation in a subrenal capsule assay at a frequency of 90% (9/10; Supplementary Methods and Supplementary Fig. 1) and the expression of dentin sialoprotein and amelogenin mRNA could not be detected (data not shown). These results suggest that CD29 is essential for the epithelial-mesenchymal interactions involved in tooth organogenesis. Hence, our present method is also a useful model system for the analysis of molecular mechanisms that function in organogenesis.

We next examined whether a bioengineered primordial organ replicates the tooth organogenesis observed in embryonic development<sup>4–6</sup>. We analyzed the expression profile of the gene networks that regulate the early development of our bioengineered tooth germ into multiple teeth (Fig. 1d,e). The multiple enamel



evidence that our present tooth germ model reproduces the interaction between epithelial and mesenchymal cells in early tooth organogenesis. These results also suggested that the cell compartmentalization, which mimics multicellular assembly and equilibrium configuration between epithelial and mesenchymal cells, is effective for the initiation of organogenesis in an artificially bioengineered organ primordium.

To examine the potential application of this bioengineering technique to the reorganization of other ectodermal organs, we examined the reconstitution of epithelium- and mesenchyme-derived single cells isolated from whisker follicles of ED14.5 mice with positive results (Supplementary Note and Supplementary Fig. 4 online).

Finally, we examined if either a bioengineered tooth germ or a developing tooth in a subrenal capsule could be successfully transplanted and redevelop in a tooth cavity after the extraction of a mandibular incisor in an 8-week-old adult mouse (Fig. 2a and Supplementary Methods). We allowed bioengineered teeth to develop in a subrenal capsule for 2 weeks and bioengineered tooth germ to develop in organ culture for 2 d. We dissected individual teeth and primordia from each culture and determined their mean length to be  $1.5 \pm 0.3$  mm (Fig. 2b) and  $250 \pm 50$   $\mu$ m (Fig. 2c), respectively. The individual primordia could generate a single tooth after 14-d culture in a subrenal capsule or *in vitro* (Supplementary Fig. 5 online). Just after dissection, we engrafted these individual bioengineered teeth or primordia into the tooth cavities in a cusp-to-root direction. In a nontransplant control experiment, we could not detect the incisor in the cavity, and we observed prominent ossification and cell infiltration (Fig. 2d). At 14 d after transplantation both the single primordia isolated from cultured tooth germ and the single teeth isolated from explants in the subrenal capsules developed in the tooth cavities and formed a correct tooth structure comprising enamel, dentin, root, dental pulp, blood vessels and bone by histological observations at frequencies of 17/22 and 23/27, respectively (Fig. 2d). The lengths of each of the bioengineered teeth developed from either tooth or tooth germ were found to be  $1.6 \pm 0.3$  mm (1.1-fold increase in length) or  $2.0 \pm 0.5$  mm (8.0-fold increase in length), respectively. Moreover, the transplantation of explants reconstituted in combination with normal epithelial cells and GFP-transgenic mouse-derived mesenchymal cells clearly demonstrated that the bioengineered tooth had developed from the explants in the cavity (Supplementary Fig. 5 online).

Periodontal ligaments could also be partially observed in the areas around the dentin in the explants (Fig. 3). Blood vessels and nerve fibers were also detectable in the pulp of not only an incisor isolated from 3 day-post-birth mice (normal) but also the developing bioengineered tooth (explant) in the oral cavity by immunohistochemical analysis with antibodies against von Willebrand factor and neurofilament-H, respectively (Fig. 3). These results indicate that both bioengineered tooth germ and teeth reconstituted by single cell-processing are transplantable, and the bioengineered tooth germ can develop a normal tooth with a complete structure. Furthermore, these data also strongly suggest

that the replacement of biological and functional teeth is possible by reconstitution in the tooth cavity of an adult animal.

It has been expected that reconstitution of an entire organ from a single cell would be required to allow regenerative therapy in addition to stem cell transplantation<sup>1–3</sup>. Our reconstituted tooth germ generates a complete and entirely bioengineered tooth, not only in *in vitro* organ cultures, but also in a tooth cavity *in vivo* after the extraction of a mandibular incisor followed by the transplantation of either early primordia or a tooth that had partially developed in a subrenal capsule. This study thus provides the first evidence of a successful reconstitution of an entire organ via the transplantation of bioengineered material. Our results therefore make a substantial contribution to the development of bioengineering technologies and the future reconstitution of primordial organs *in vitro*. Our present findings should also encourage the future development of organ replacement by regenerative therapy.

*Note: Supplementary information is available on the Nature Methods website.*

#### ACKNOWLEDGMENTS

We thank M. Okabe (Osaka University) for providing the C57BL/6-TgN (act-EGFP) OsbC14-Y01-FM131 mice. We are also grateful to K. Itoh and M. Sugai (Kyoto University) for critical reading of this manuscript. We also thank to T. Katakai (Kyoto University) and Y. Nishi (Nagahama Institute of Bioscience and Technology) for their valuable discussions and encouragement. This work was partially supported by an "Academic Frontier" Project for Private Universities to Y.T. and T.T. (2003–2007) and by a Grant-in Aid for Scientific Research in Priority Areas (50339131) to T.T. from MEXT Japan.

#### AUTHOR CONTRIBUTIONS

K.N. was involved in each of the experiments described in this study. R.M. analyzed the explants that were formed by a combination of normal and GFP-transgenic mouse-derived cells and performed the immunohistochemical analysis shown in Figure 3. Y.S. performed and analyzed the transplantation experiments in both the subrenal capsule and the tooth cavity. K.I. and M.S. performed the *in situ* hybridization analysis. Y.T. performed the subrenal capsule transplantation experiments and histological analysis. M.O. maintained the *in vitro* organ cultures and performed whole-mount analysis of the chimeric bioengineered tooth germ. K.N. and T.T. prepared the manuscript. K.N., M.S., Y.T. and T.T. discussed the results and also contributed to the preparation of this manuscript. T.T. designed the experiments.

#### COMPETING INTERESTS STATEMENT

The authors declare that they have no competing financial interests.

Published online at <http://www.nature.com/naturemethods/>  
Reprints and permissions information is available online at  
<http://npg.nature.com/reprintsandpermissions>

1. Langer, R.S. & Vacanti, J.P. *Sci. Am.* **280**, 86–89 (1999).
2. Brookes, J.P. & Kumar, A. *Science* **310**, 1919–1923 (2005).
3. Atala, A. *Expert Opin. Biol. Ther.* **5**, 879–892 (2005).
4. Pispas, J. & Thesleff, I. *Dev. Biol.* **262**, 195–205 (2003).
5. Thesleff, I. *J. Cell Sci.* **116**, 1647–1648 (2003).
6. Tucker, A. & Sharpe, P. *Nat. Rev. Genet.* **5**, 499–508 (2004).
7. Sharpe, P.T. & Young, C.S. *Sci. Am.* **293**, 34–41 (2005).
8. Young, C.S. *et al. J. Dent. Res.* **81**, 695–700 (2002).
9. Ohazama, A., Modino, S.A., Miletich, I. & Sharpe, P.T. *J. Dent. Res.* **83**, 518–522 (2004).
10. Song, Y. *et al. Dev. Dyn.* **235**, 1334–1344 (2006).
11. Hu, B. *et al. Tissue Eng.* **12**, 2069–2075 (2006).
12. Steinberg, M.S. *Dev. Biol.* **180**, 377–388 (1996).
13. Hata, R.I. *Cell Biol. Int.* **20**, 59–65 (1996).
14. Salmivirta, K., Gullberg, D., Hirsch, E., Altruda, F. & Ekblom, P. *Dev. Dyn.* **205**, 104–113 (1996).



## Supplementary Information

### Supplementary Notes

**Analysis of the Development of a Chimeric Bioengineered Tooth Germ in *in Vitro* Organ Culture.** We investigated whether our current bioengineered tooth germ is reconstituted by completely dissociated single cells from both epithelial and mesenchymal tissues of incisor tooth germ. We developed a chimeric bioengineered tooth germ analysis using the single cells dissociated from tooth germs of normal and GFP-transgenic mice. Each dissociated cells of epithelial and mesenchymal cells of normal or GFP-transgenic mice were prepared as described (see **Supplementary Methods**). At first, we analyzed the development of the chimeric bioengineered tooth germ reconstituted between normal mice-derived epithelial cells and the mixed mesenchymal cells isolated from normal and GFP-transgenic mice with cell compartmentalization at high-cell density. The mesenchymal cells were premixed with normal and GFP-transgenic mice-derived cells at the chimerism of 95% and 5%, respectively (see **Supplementary Fig. 1**). Whereas the green fluorescence could not be detected in epithelial cell-derived ameloblast, the fluorescence was observed and distributed in dental mesenchymal-derived cell types, pulp and odontoblast. The number of GFP-positive cells correlated to the chimerism between normal and GFP transgenic mice-derived cells in this chimeric tooth germ (data not shown). Furthermore, we also examined the chimeric germ reconstituted between epithelial and mesenchymal cells each containing of equally number of normal and GFP-transgenic mice-derived single cells with cell compartmentalization at high-cell density (see **Supplementary Fig. 1**). GFP-positive cells largely distributed in the bioengineered tooth according to the chimerism and detected in the all cell types of ameloblast, pulp and odontoblast. These results indicate that our current tooth germ method successfully reconstituted by single cell manipulation.

**Multiple Tooth Induction in a Bioengineered Incisor Tooth Primordium by Gene Expressions of Signalling Network.** We analyzed the expression profile of signalling networks that play essential roles both in early tooth development and in morphogenesis<sup>1,2</sup>. The expression of the enamel knot marker genes<sup>3</sup>, Shh and Wnt10b, were detectable in plural sites and at the boundary surface between epithelial and mesenchymal cells in our bioengineered incisor tooth germ (see **Supplementary Fig. 3**). Activin  $\beta$ A and Fgf3 transcripts were also mainly detectable in the mesenchyme that had formed in the region adjacent to the epithelial Shh-expression site (see **Supplementary Fig. 3**). Msx1 transcript was additionally observed throughout the entire mesenchyme, as seen in normal tooth germ (see **Supplementary Fig. 3**).

Ectodin inhibits the expression of p21, through its antagonistic effects upon BMP4 signalling and is critical for the spatial delineation of enamel knots and cusps<sup>4,5,6</sup>. Consistent with this, Ectodin and p21 were found to be inversely expressed at the boundary surfaces between the epithelial and mesenchymal cells (see **Supplementary Fig. 3**). Furthermore, the signalling between ectodysplasin (Eda) and its receptor, Edar, is thought to induce enamel knot formation<sup>7</sup> and the expression pattern of Edar was identical to those of Shh and p21 in the reconstituted tooth germ (see **Supplementary Fig. 3**).

The Shh signalling network molecules, patched 1 (Ptc1) and growth arrest-specific gene (Gas1) are thought to regulate the regionalization of the odontogenic mesenchyme in the mandibular arch<sup>8</sup>. Ptc1 and Gas1 transcripts were detectable in the proximal and distal mesenchyme, respectively, of the boundary surface between the epithelium and mesenchyme, and the strong expression of Ptc1 transcripts could be observed in the regions adjacent to the enamel knot (see **Supplementary Fig. 3**). These observations are clearly indicated the evidences that our current tooth germ model reproduce the interaction between epithelial and mesenchymal cells in early tooth organogenesis.

**Generation of a Reconstituted Whisker from a Bioengineered Follicle.** We investigated whether it would be possible to a bioengineered mouse whisker using our developed bioengineering technology for the reconstitution of artificial primordial organs. Tissues containing whisker follicles were dissected from the cheeks of ED14.5 mice and the epithelial and mesenchymal tissues were completely dissociated to single cells via the same enzymatic method used for tooth germ regeneration (see **Supplementary Fig. 1**). Epithelial and mesenchymal cells were also reconstituted with cell compartmentalization at a high-cell density in a collagen gel, and the bioengineered whisker follicle was transferred to a cell culture insert. After one day of incubation, the explant was then transplanted into a subrenal capsule for 14 days (see **Supplementary Fig. 4**). At post-transplantation day 14, the explants in the subrenal capsule were found to regenerate a whisker at a 100% frequency (20/20; see **Supplementary Fig. 4**). Histological analysis of these explants also revealed the expected tissue morphologies, such as the whisker shaft (ws), inner root sheath (irs) and outer root sheath (ors). Moreover, these tissues were arranged normally, when compared with a natural whisker (see **Supplementary Fig. 4**).

### Reference

1. Tucker, A. & Sharpe, P. The cutting-edge of mammalian development; how the embryo makes teeth. *Nat Rev Genet* **5**, 499-508 (2004).
2. Thesleff, I. Epithelial-mesenchymal signalling regulating tooth morphogenesis. *J Cell Sci* **116**, 1647-1648 (2003).
3. Aberg, T. et al. Runx2 mediates FGF signaling from epithelium to mesenchyme during tooth morphogenesis. *Dev Biol* **270**, 76-93 (2004).
4. Laurikkala, J., Kassai, Y., Pakkasjarvi, L., Thesleff, I. & Itoh, N. Identification of a secreted BMP antagonist, ectodin, integrating BMP, FGF, and SHH signals from the tooth enamel knot. *Dev Biol* **264**, 91-105 (2003).
5. Jernvall, J., Aberg, T., Kettunen, P., Keranen, S. & Thesleff, I. The life history of an embryonic signaling center: BMP-4 induces p21 and is associated with apoptosis in the mouse tooth enamel knot. *Development* **125**, 161-169 (1998).
6. Kassai, Y. et al. Regulation of mammalian tooth cusp patterning by ectodin. *Science* **309**, 2067-2070 (2005).
7. Tucker, A.S. et al. Edar/Eda interactions regulate enamel knot formation in tooth morphogenesis. *Development* **127**, 4691-4700 (2000).
8. Cobourne, M.T., Miletich, I. & Sharpe, P.T. Restriction of sonic hedgehog signalling during early tooth development. *Development* **131**, 2875-2885 (2004).

## Supplementary Methods

### Animals

C57BL/6 mice were purchased from CLEA Japan Inc (Tokyo, Japan). C57BL/6-TgN (act-EGFP) OsbC14-Y01-FM131 mice were obtained from RIKEN Bioresource Center (Tsukuba, Japan). Mouse care and handling conformed to the NIH guidelines for animal research. All experimental protocols were approved by the Tokyo University of Science Animal Care and Use Committee.

### Reconstitution of bioengineered primordial organs from single cells

Tooth germs derived from incisors or molars were dissected from the mandibles of ED14.5 mice. The extra tissues surrounding of tooth germ should be carefully removed. The purity of tooth germ cells affect to the frequency of tooth formation. Isolated tooth germs were incubated in 1.2 U/ml dispase II (Roche, Mannheim, Germany) and 20 U/ml DNase I (Takara Bio, Shiga, Japan) for 12.5 min at room temperature. The epithelial and mesenchymal tissues were separated using a fine needle. The epithelial tissues were treated twice at 37°C for 20 min in 100 U/ml collagenase I (Worthington, Lakewood, NJ)-PBS(-), then in Ca<sup>2+</sup>- and Mg<sup>2+</sup>-phosphate-buffered saline (PBS(-)) supplemented with 0.25% trypsin (Sigma, St. Louis, MO) and 20 U/ml DNase I (Takara Bio) for 5 min at 37°C, and dissociated into single cells by gentle pipetting. Single cells of mesenchymal origin were also prepared by treatment with PBS(-) supplemented with 0.25% trypsin (Sigma), 50 U/ml collagenase I, and 20 U/ml DNase I (Takara Bio) at 37°C for 10 min. Each epithelial and mesenchymal cells were precipitated by centrifugation in a siliconised microtube and the supernatant was removed completely using a GELoader Tip 0.5-20 µl (Eppendorf, Hamburg, Germany). The cell density of the precipitated epithelial and mesenchymal cells after the removal of supernatants reached at the concentration of 5 × 10<sup>8</sup> cells/ml. We defined the cell concentration (5 × 10<sup>8</sup> cells/ml) as a "high-cell density". To prepare bioengineered primordial organs with the correct cell compartmentalization between the epithelial and mesenchymal cells at a high-cell density (5 × 10<sup>8</sup> cells/ml), the precipitated mesenchymal cells were mixed without further dilution and injected (0.2 µl) using 0.1-10 µl pipette tip (Molecular Bio Products, San Diego, CA) into a 30 µl gel drop of Cellmatrix type I-A (Nitta gelatin, Osaka, Japan), which is acid-soluble collagen isolated from tendon of pig, formed on a siliconised dish. Epithelial single cells were then mixed without further dilution and injected (0.1-0.2 µl) into an area adjacent to the mesenchymal cell aggregate to enable direct cell contact (Fig. 1a). To prepare bioengineered tooth germ without cell compartmentalization between the epithelial and mesenchymal cells at a high-cell density (5 × 10<sup>8</sup> cells/ml), the cell suspensions of epithelial and mesenchymal cells were premixed and precipitated. The cell precipitate were mixed and injected (0.3-0.4 µl) into a collagen gel drop. The bioengineered tooth germs were incubated for 5 min at 37°C, placed on a cell culture insert (0.4 µm pore diameter; BD, Franklin Lakes, NJ), and the explants were then incubated at 37°C in a humidified atmosphere of 5% CO<sub>2</sub>. For the neutralization of CD29, each epithelial and mesenchymal cell preparation were preincubated with 100 µl of

50 µg/ml of an anti-CD29 monoclonal antibody (αCD29 mAb; clone 9EG7, BD, San Diego, CA) in PBS(-) in the absence of NaN<sub>3</sub>. The reconstituted tooth germ was prepared in collagen gel containing 50 µg/ml of αCD29 mAb. The explants were then subjected to a subrenal capsule assay as described below.

### Organ cultures

Reconstituted explants were cultured for 2 days for up to 14 days on cell culture inserts in 12-well cell culture plates (BD) containing 380 µl/well Dulbecco's modified eagle medium (DMEM; Sigma) supplemented with 10% FCS (JRH), 100 µg/ml ascorbic acid (Sigma), 2 mM L-glutamine (Sigma). Cultures were incubated at 37°C in a humidified atmosphere of 5% CO<sub>2</sub> and the culture medium was changed at 2-day intervals.

### Subrenal Capsule Assays

After 2 days cultivation, the reconstituted germs of tooth or whisker follicles were transplanted into a subrenal capsule for 14 days using 8 week-old male mice as the host, according to the method of Bogden and co-workers<sup>1</sup>.

### Tissue Preparation and Immunohistochemistry

The tissues were removed and immersed in 4% paraformaldehyde in PBS(-). After fixation, the tissues were decalcified in 4.5% EDTA (pH 7.4) for 1-10 days at 4°C. To store frozen samples, the specimens were immersed in a series of graded sucrose solutions and embedded in Tissue-Tek O.C.T. (Sakura-Finetek USA, Torrence, CA). For immunohistochemistry, the primary antibodies used were anti von Willibrand factor (αvWF pAb; 1:100, Chemicon, Temecula, CA)<sup>2</sup> and anti-neurofilament H (αNF-H pAb; 1:100, Chemicon)<sup>3</sup> polyclonal antibodies. Immunoreactivity was detected using fluorescence-conjugated goat anti-rabbit IgG (1:200, Chemicon). The sections were observed using an Axio Imager A1 (Carl Zeiss, Jena, Germany) with an AxioCAM MRc5 (Carl Zeiss) and processed with AxioVision software (Carl Zeiss). Fluorescent images were acquired using an Axiovert 200M (Carl Zeiss) with an AxioCAM MRm (Carl Zeiss).

### In Situ Hybridization Analysis

*In situ* hybridizations were performed using 10 µm frozen sections. Digoxigenin-labelled probes for specific transcripts were prepared by PCR with primers designed using published sequences (GenBank Accession Numbers; Shh: NM009170, Msx1: NM010835, Fgf3: NM008007, Wnt10b: NM011718, Activin βA: NM008380, Periostin: NM015784, Amelogenin: NM009666, Dspp: NM010080, Ectodin: NM025312, Edar: NM010100, p21: NM007669, Ptc1: NM008957, Gas1: NM008086). After hybridization, the expression patterns for each mRNA were detected and visualized by immunoreactivity with an anti-digoxigenin alkaline phosphatase-conjugated Fab fragments (Roche), according to the method of Iseki and co-workers<sup>4</sup>.

### Transplantation

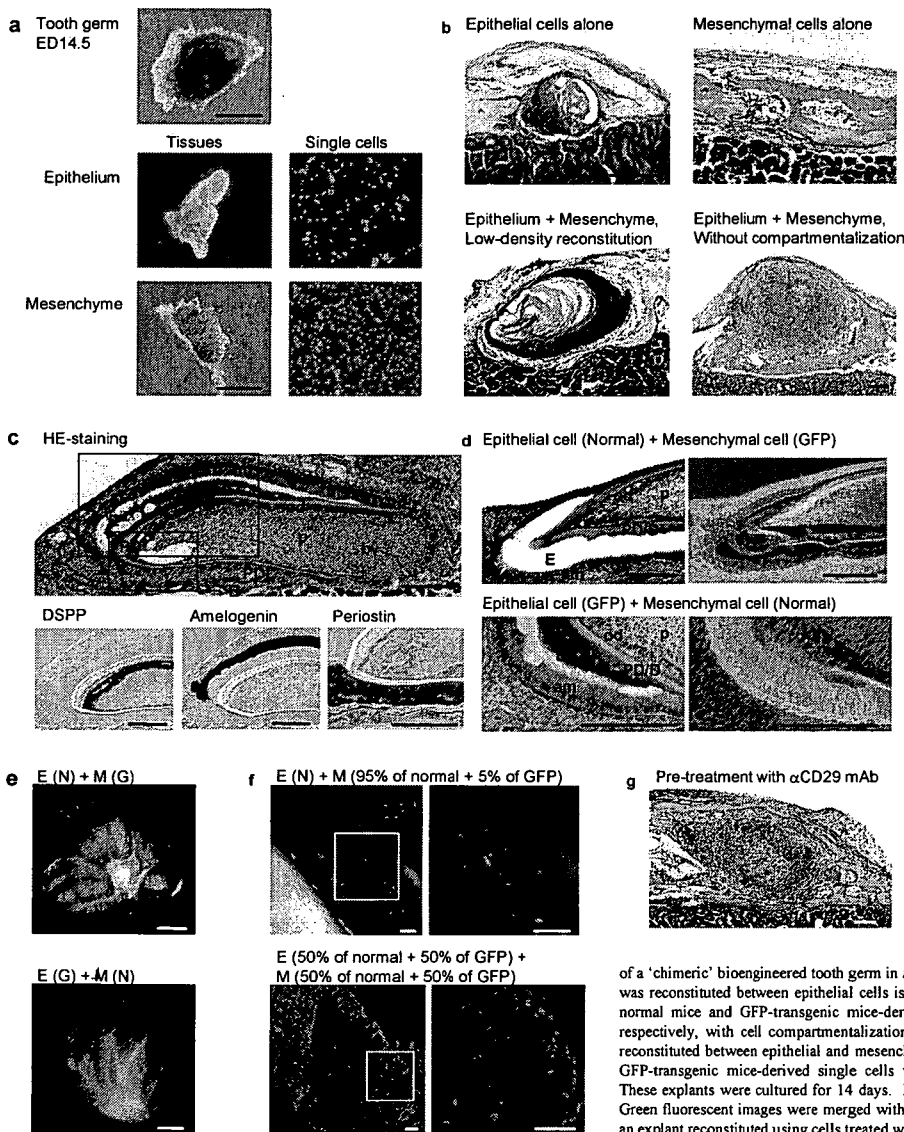
After incubation, reconstituted explants were separated into the individual primordium using a fine needle. The mandibular bones around the right incisors of 8 week-old adult male mice were surgically removed and the right incisors were then



extracted under deep anaesthesia. After 3 days, the vestibular surface of the right mandibular ramus was surgically exposed also under deep anaesthesia. An incision of about 8 mm in length was then made through the skin with a fine scissors to access the muscle layer, according to an imaginary line joining the auditory meatus to the lip commissure. The fibres of the masseter were separated along their longitudinal axis with a scalpel blade. The underlying bony surface of the ramus was then exposed and a scalpel blade was used to create a hole through the alveolar bone. The bony window was placed approximately 2 mm anterior to the posterior border of the ramus and slightly superior to the bony elevation at the apical end of the incisor. A sample was then inserted through the bony window. The animals were then sutured and the surgical site was cleaned.

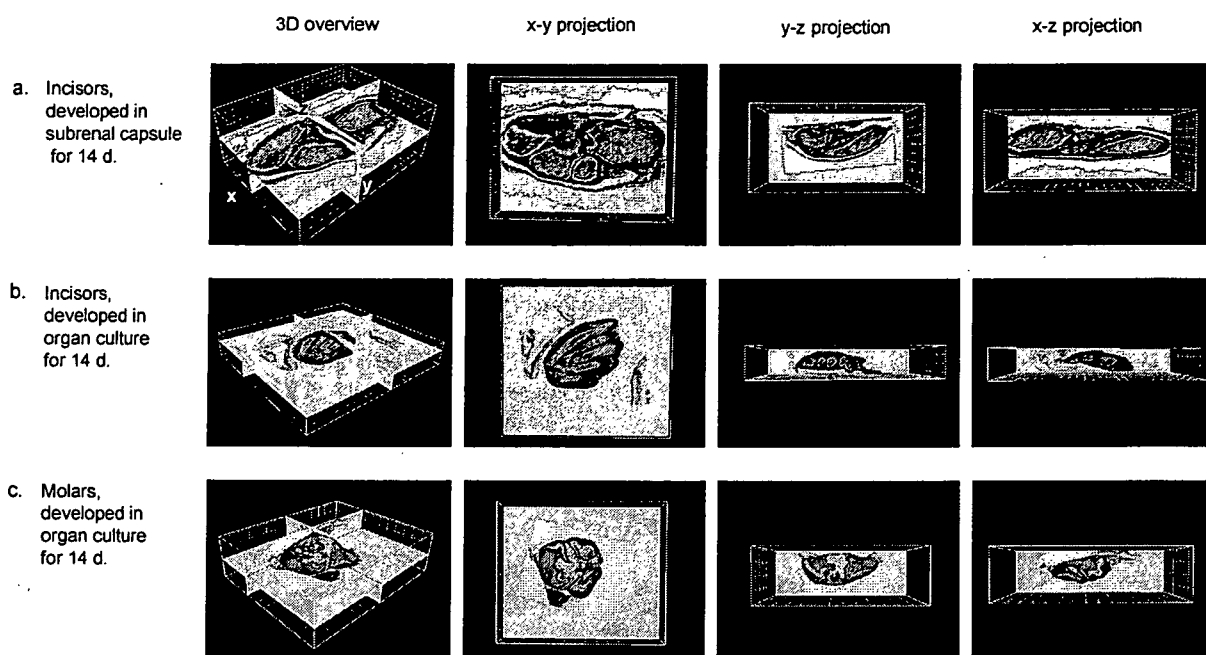
## References

1. Fingert, H.J., Treiman, A. & Pardee, A.B. Transplantation of human or rodent tumors into cyclosporine-treated mice: a feasible model for studies of tumor biology and chemotherapy. *Proc Natl Acad Sci U S A* **81**, 7927-7931 (1984).
2. Grunewald, M. et al. VEGF-induced adult neovascularization: recruitment, retention, and role of accessory cells. *Cell* **124**, 175-189 (2006).
3. Westenbroek, R.E., Anderson, N.L. & Byers, M.R. Altered localization of Cav1.2 (L-type) calcium channels in nerve fibers, Schwann cells, odontoblasts, and fibroblasts of tooth pulp after tooth injury. *J Neurosci Res* **75**, 371-383 (2004).
4. Iseki, S. et al. Fgfr2 and osteopontin domains in the developing skull vault are mutually exclusive and can be altered by locally applied FGF2. *Development* **124**, 3375-3384 (1997).

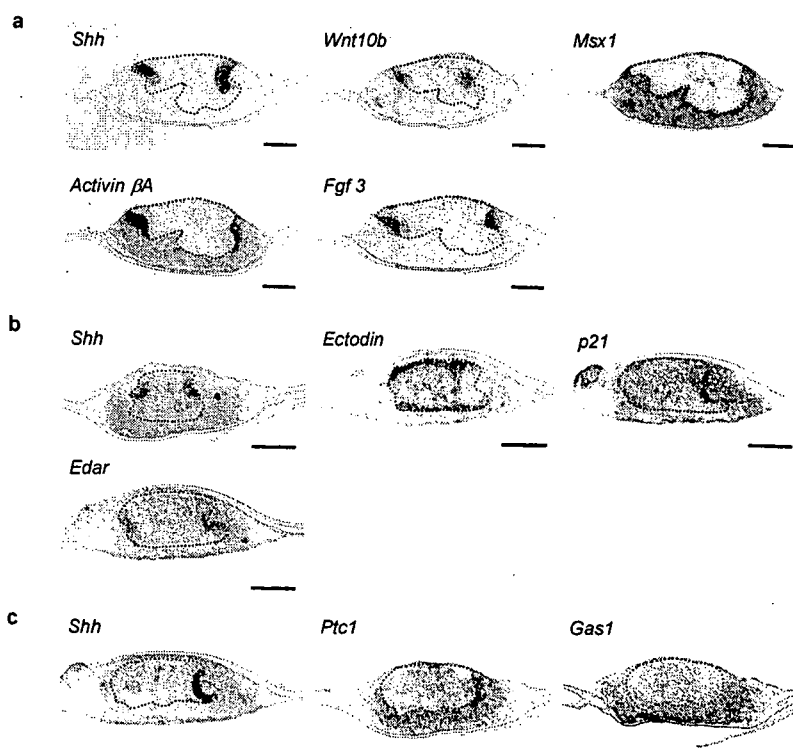


**Supplementary Fig. 1** Effects of cell density and cell compartmentalization between epithelial and mesenchymal cells upon the generation of bioengineered teeth. (a) Phase contrast images of tooth germ, tissues and dissociated single cells as described (see Supplementary Methods). Scale bar, 200  $\mu$ m. (b) Histological analysis of the explants under various conditions. The reconstituted tooth germs were prepared from epithelial cells only (upper left), mesenchymal cells only (upper right), a combination of epithelial and mesenchymal cells showing compartmentalization at a low-cell density (lower left) and a combination of epithelial and mesenchymal cells in the absence of compartmentalization at a high-cell density (lower right). For the preparation of a low-density reconstituted structure, the cells were suspended in medium of four volumes to the packed cell volume. To prepare tooth germ in the absence of compartmentalization between the epithelial and mesenchymal cells, an equal number of each cell type was premixed, followed by reconstitution. The reconstituted germs were grown for 2 days by *in vitro* organ culturing and then subjected to the subrenal capsule assay. Scale bar, 200  $\mu$ m. (c) Histological analysis of the expression of typical differentiation markers for ameloblasts, odontoblasts and periodontal ligaments in a bioengineered incisor at post-transplantation day 14 in the subrenal capsule. The regenerated tooth displays normal cellular and tissue components in the correct location, including ameloblasts (am), odontoblasts (od), pulp cells (p), blood vessels (bv), enamel (E), dentin (D), pre-dentin (PD), periodontal ligaments (PDL) and alveolar bone (B). Gene expression patterns were detected by *in situ* hybridization of sequential sections of bioengineered incisor. Scale bar, 250  $\mu$ m. (d) Analysis of the cell types that have differentiated from the epithelial and mesenchymal cells in the bioengineered incisor tooth germ. The origins of the epithelial and mesenchymal cells are indicated above the panels. Green fluorescent images were merged with DIC images. The abbreviations used are identical to those shown in (c). Scale bar, 250  $\mu$ m. (e) Wholemount analysis of bioengineered tooth germ, which was reconstituted using a combination of epithelial (E) or mesenchymal cells (M) isolated from normal mice (N) or GFP-transgenic mice (G), and cultured for 4 days. The origins of the epithelial and mesenchymal cells are indicated above each panel. Green fluorescent images were merged with those of DIC. Images were acquired using a STEREO Lumor V12 (Carl Zeiss). Scale bar, 200  $\mu$ m. (f) Analysis of development of a 'chimeric' bioengineered tooth germ in *in vitro* organ culture. The chimeric bioengineered tooth germ was reconstituted between epithelial cells isolated from normal mice and mesenchymal cells mixed with normal mice and GFP-transgenic mice-derived mesenchymal cells at the chimerism of 95% and 5%, respectively, with cell compartmentalization at high-cell density (upper). The chimeric tooth germ was reconstituted between epithelial and mesenchymal cells each containing of equally number of normal and GFP-transgenic mice-derived single cells with cell compartmentalization at high-cell density (lower). These explants were cultured for 14 days. Images were acquired using a LSM 510 META (Carl Zeiss). Green fluorescent images were merged with those of DIC. Scale bar, 50  $\mu$ m. (g) Histological analysis of an explant reconstituted using cells treated with CD29 antibodies. Scale bar, 200  $\mu$ m.

## BRIEF COMMUNICATIONS

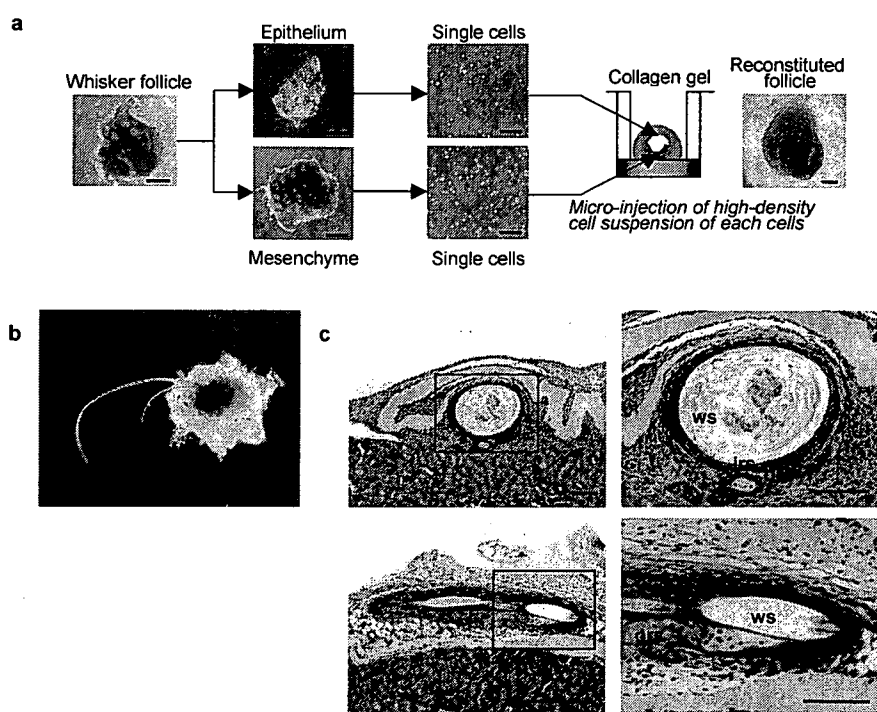


**Supplementary Fig. 2** Three-dimensional histological analysis of bioengineered teeth under various developmental conditions. Bioengineered incisors developed in a subrenal capsule (a), via *in vitro* organ culturing (b), bioengineered molars developed via *in vitro* organ culturing (c) were sectioned and stained with haematoxylin-eosin. The sections were then observed by an Axio Imager A1 (Carl Zeiss, Jena, Germany) with an AxioCAM MRc5 (Carl Zeiss) and processed with AxioVision software (Carl Zeiss). Serial images were compiled and aligned using an LSM 5 Image Browser (Carl Zeiss) and AutoAligner (Bitplane AG, Zurich, Switzerland), and analyzed using Imapris 4 software (Carl Zeiss). A three-dimensional overview, x-y projection, y-z projection and x-z projection are demonstrated.

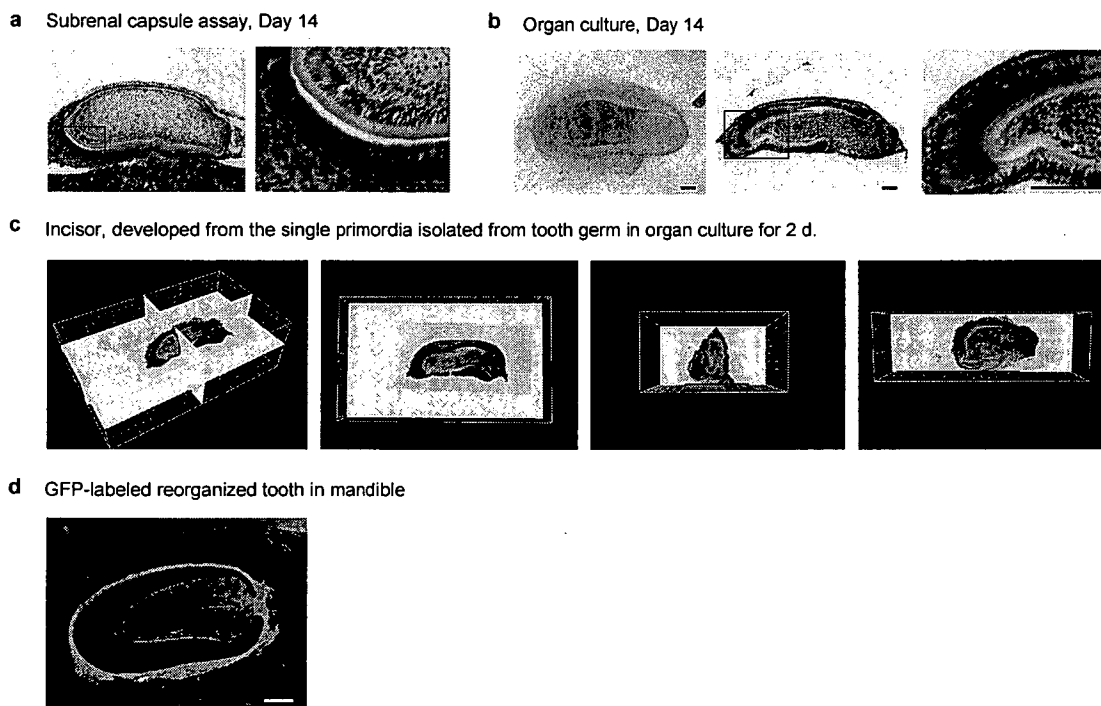


**Supplementary Fig. 3** Expression of the regulatory genes that function during early tooth development in a bioengineered incisor tooth germ. Gene expression in bioengineered incisor tooth germ that had been cultured *in vitro* for 2 days was detected by *in situ* hybridization. Dotted lines indicate the interface between the epithelial and mesenchymal cells and the inside of the lined areas indicate the epithelial cell aggregates. Scale bar, 200  $\mu$ m. (a) Expression analysis of enamel knot and mesenchymal cell markers. *Shh*, *Wnt10b*, *Msx1*, *Activin  $\beta$ A* and *Fgf3* transcripts are detectable in sequential sections. (b) *In situ* hybridization analysis of genes associated with the induction of the enamel knot in bioengineered tooth germ. mRNAs for *Shh*, *Ectodin*, *p21* and *Edar* were analyzed in sequential sections of the explant. (c) Analyses of *Shh*-signaling related genes that function in the regionalization of odontogenic and non-odontogenic mesenchyme. *Ptc1* and *Gas1* transcripts are detectable in sequential sections of reconstituted tooth germ.





**Supplementary Fig. 4** Generation of a reconstituted whisker *in vivo* from a bioengineered follicle. (a) Schematic representation of the bioengineering method employed for the reconstitution of a whisker follicle *in vitro*. Scale bar, 250  $\mu\text{m}$ . (b) Whole mount analysis of a bioengineered whisker following a subrenal capsule transplant for 14 days. Scale bar, 250  $\mu\text{m}$ . (c) Histological analysis of a bioengineered whisker following a subrenal capsule transplant for 14 days. Abbreviations: ws, whisker shaft; irs, inner root sheath; ors, outer root sheath. Scale bar, 100  $\mu\text{m}$ .



**Supplementary Fig. 5** Development and transplantation of individual primordia. (a) *In vivo* and (b) *in vitro* development of individual primordia, regenerated either in a subrenal capsule or by *in vitro* organ culture, both for 14 days. Boxes indicate the area shown by higher magnification in the right hand panels. Scale bar, 100  $\mu\text{m}$ . (c) Bioengineered single incisor developed from a dissected single primordium via *in vitro* organ culturing for 2 days were sectioned and stained with haematoxylin-eosin. The sections were then observed by an Axio Imager A1 (Carl Zeiss, Jena, Germany) with an AxioCAM MRc5 (Carl Zeiss) and processed with AxioVision software (Carl Zeiss). Serial images were compiled and aligned using an LSM 5 Image Browser (Carl Zeiss) and AutoAligner (Bitplane AG, Zurich, Switzerland), and analyzed using Imaris 4 software (Carl Zeiss). A three-dimensional overview, x-y projection, y-z projection and x-z projection are demonstrated. (d) Transplantation of bioengineered incisor tooth germ reconstituted by a combination of normal and GFP-transgenic mouse epithelial cells and mesenchymal cells. GFP fluorescent and DIC images were merged. Scale bar, 200  $\mu\text{m}$ .

## **PRESS RELEASE BY NATURE**

February 13, 2007

**Katherine Anderson, Nature London  
Nature Publishing Group**

*Within this release, a few papers of particular newsworthiness are highlighted, with author contact details, and the rest are listed. Journalists are also given online access to the papers, so they can follow up stories of interest.*

### **A method to regrow teeth**

DOI: 10.1038/nmeth1012

Scientists have for the first time successfully replaced natural teeth in mice with teeth that were created in a Petri dish from single cells. The experiment is described online this week in Nature Methods. Takashi Tsuji and colleagues started with the two cell types that develop into a tooth -mesenchymal and epithelial cells. First they grew each cell type separately to get larger quantities of cells and then injected them into a drop of collagen - a substance which 'glues' cells together in an organism. The cells developed into a budding tooth with high efficiency, and when transplanted into the cavity of an extracted tooth in a mouse developed normally and showed the same composition and structure as natural teeth. The authors provide further evidence that this method can be applied to any organ that develops from these cell types by regrowing a follicle that eventually forms a whisker in a mouse.

**Author contact:**

Takashi Tsuji (Tokyo University of Science, Chiba, Japan)

Tel: +81 4 7122 9711; E-mail: [t-tsuji@nifty.com](mailto:t-tsuji@nifty.com)

*Please note that the press release has already been distributed and this copy is for information purposes only. Providing authors with a copy of their press release entry is a new service. Please tell us what you think of it by emailing us at [press@nature.com](mailto:press@nature.com)*

ORIGINAL ARTICLE

Takashi Yamashiro · Li Zheng · Yuko Shitaku ·  
Masahiro Saito · Takanori Tsubakimoto · Kenji  
Takada · Teruko Takano-Yamamoto · Irma Thesleff

## Wnt10a regulates dentin sialophosphoprotein mRNA expression and possibly links odontoblast differentiation and tooth morphogenesis

Received July 23, 2006; accepted in revised form October 13, 2006

**Abstract** We have explored the role of Wnt signaling in dentinogenesis of mouse molar teeth. We found that Wnt10a was specifically associated with the differentiation of odontoblasts and that it showed striking colocalization with dentin sialophosphoprotein (Dspp) expression in secretory odontoblasts. Dspp is a tooth specific non-collagenous matrix protein and regulates dentin mineralization. Transient overexpression of Wnt10 in C3H10T1/2, a pluripotent fibroblast cell line induced Dspp mRNA. Interestingly, this induction occurred only when transfected cells were cultured on Matrigel basement membrane extracts. These findings indicated that Wnt10a is an upstream regulatory mol-

ecule for Dspp expression, and that cell–matrix interaction is essential for induction of Dspp expression. Furthermore, Wnt10a was specifically expressed in the epithelial signaling centers regulating tooth development, the primary and secondary enamel knots. The spatial and temporal distribution of Wnt10a mRNA demonstrated that the expression shifts from the secondary enamel knots, to the underlying preodontoblasts in the tips of future cusps. The expression patterns and overexpression studies together indicate that Wnt10a is a key molecule for dentinogenesis and that it is associated with the cell–matrix interactions regulating odontoblast differentiation. We conclude that Wnt10a may link the differentiation of odontoblasts and cusp morphogenesis.

Takashi Yamashiro · Yuko Shitaku · Kenji Takada  
Department of Orthodontics and Dentofacial Orthopedics  
Graduate School of Dentistry  
Osaka University, 1-8 Yamadaoka, Suita  
Osaka 565-0871, Japan

**Key words** odontoblast · Dspp · Wnt10a ·  
dentinogenesis · tooth

Takashi Yamashiro (✉) · Li Zheng ·  
Teruko Takano-Yamamoto  
Department of Orthodontics and Dentofacial Orthopedics  
Graduate School of Medicine and Dentistry  
Okayama University, 2-5-1 Shikata-cho  
Okayama 700-8558, Japan  
Tel: +81 86 2356690  
Fax: +81 86 2356694  
E-mail: yamataka@md.okayama-u.ac.jp

Takashi Yamashiro · Irma Thesleff  
Developmental Biology Programme, Institute of  
Biotechnology, University of Helsinki, Helsinki 00014, Finland

Masahiro Saito · Takanori Tsubakimoto  
Department of Oral Medicine  
Division of Operative Dentistry and Endodontics  
Kanagawa Dental College  
82 Inaoka-cho, Yokosuka  
Kanagawa 238-8580, Japan

### Introduction

Dentin is one of the three mineralized tissues of the tooth, and it is produced by odontoblasts differentiating from dental papilla mesenchymal cells. Dentin is very similar to bone in its matrix protein composition. However, whereas bone remodels throughout postnatal life and participates in calcium homeostasis, dentin, once formed, does not undergo remodeling. On the other hand, it can respond to injury or stimulation by forming reparative dentin to protect the dental pulp (Linde and Goldberg, 1993). Unlike osteoblast differentiation, the differentiation of odontoblasts is regulated by epithelial–mesenchymal interactions, which instruct both tooth morphogenesis and cell differentiation (Thesleff et al., 1989, 1991; Thesleff and Aberg, 1999). Recombination experiments of the dissociated developing dental

tissues have shown that odontoblast differentiation is controlled by the inner dental epithelium (Ruch et al., 1982; Kollar, 1985; Thesleff et al., 1989). Odontoblasts are columnar polarized cells with eccentric nuclei and long cellular processes, and this cytological polarization specifically occurs in a single cell layer adjacent to the basement membrane of the inner dental epithelium (Linde and Goldberg, 1993). The terminal differentiation of odontoblasts is initiated during the bell stage of tooth morphogenesis at the sites of the future cusps (Lesot et al., 2001; Thesleff et al., 2001). The patterning of the cusps, on the other hand, is determined by the positions of the secondary enamel knots, epithelial signaling centers resembling other embryonic signaling centers, such as the notochord and the apical ectodermal ridge in limbs (Jernvall et al., 1994; Jernvall and Thesleff, 2000). The cells of the enamel knots are non-proliferative, and they express several signaling molecules. These signals may control the folding of the inner enamel epithelium and as odontoblast differentiation starts from the mesenchymal cells underlying enamel knots it has been suggested that signals from the secondary enamel knots may also determine the location and time of the onset of odontoblast terminal differentiation (Thesleff et al., 2001). However the molecular mechanisms of the induction of odontoblast differentiation have remained unknown.

Dentin and bone share many extracellular matrix proteins associated with mineralization such as dentin matrix protein 1, fibronectin, collagen type I, alkaline phosphatase, osteonectin, osteopontin, bone sialoprotein, bono-1, and osteocalcin (Tsukamoto et al., 1992; Nakashima et al., 1994; Shiba et al., 1998; James et al., 2004). Dentin sialophosphoprotein (Dspp) is a non-collagenous extracellular matrix protein that is specifically expressed by odontoblasts (D'Souza et al., 1997). Dspp is a phosphorylated parent protein that is cleaved post-translationally into two proteins: dentin sialoprotein (Dsp) and dentin phosphoprotein (Dpp) (Feng et al., 1998). *In situ* hybridization and other experimental analyses have shown that *Dspp* is expressed predominantly in odontoblasts, transiently in preameloblasts, and at low levels in osteoblasts (D'Souza et al., 1997; Qin et al., 2002). In humans, several mutations have been identified in patients with dentinogenesis imperfecta, which is an autosomal dominant disorder of the tooth that specifically affects dentin biomineralization (Shields et al., 1973; Xiao et al., 2001; Zhang et al., 2001; Rajpar et al., 2002). A similar phenotype is found in *Dspp* null mutant mice, which feature a disturbance of dentin mineralization without any influences on bone (Sreenath et al., 2003). Hence, it is established that Dspp has a crucial role in the formation of mineralized dentin. Although the importance of epithelial-mesenchymal interactions and extracellular matrix for odontoblast differentiation is established, the molecular

mechanisms of the interactions mediating odontoblast differentiation and inducing *Dspp* expression are not known.

Wnt genes encode a large family of secreted signaling proteins that specify various cell lineage pathways in development. Wnt proteins are now recognized as one of the major families of developmentally important signaling molecules and they regulate such intriguing processes as embryonic induction, the generation of cell polarity, and the specification of cell fate (Cadigan and Nusse, 1997; Nusse, 2003). In early tooth development, several Wnt genes are expressed from the initiation stage to the early bell stage (Sarkar and Sharpe, 1999). Targeted inactivation of lymphoid enhancer factor-1 (LEF1), a nuclear mediator of Wnt signaling, results in an arrest of tooth development at the bud stage (van Genderen et al., 1994). LEF1 serves as a relay of a Wnt signal to a fibroblast growth factor signal in the enamel knot in the dental epithelium, which establishes a network of reciprocal and sequential signaling between epithelium and mesenchyme (Kratochwil et al., 2002).

Here we provide evidence that Wnt10a signaling may be involved in odontoblast terminal differentiation, and based on the expression pattern of *Wnt10a*, we suggest that it has a role in linking tooth morphogenesis and odontoblast differentiation.

## Materials and methods

### Materials

Lipofectamine Plus was obtained from Gibco BRL (Gaithersburg, MD). Biocoat Matrigel-coated dishes were from Becton Dickinson (Labware, MA). The rabbit polyclonal anti-Wnt10a antibody was produced by Sigma Genosys Co. (Hokkaido, Japan) using a synthetic peptide as antigen, which was established by the Wnt10a protein sequence analysis (U61969). The amino acid sequence of the antigen peptide is RRGDEEAFRRKLHR and corresponds to amino acids 163–176 of the Wnt10a protein. All other chemicals were analytical grade.

### Processing of tissues

Wild-type mouse embryos were obtained from the NMRI strain. Heads of embryonic E12, E13, E14, and E16 mice and postnatal 14 day old mice were dissected in Dulbecco's phosphate-buffered saline. The tissues were fixed in 4% paraformaldehyde at 4°C overnight. P14 heads were decalcified in 12.5% ethylene-diamine-tetraacetic acid (EDTA) for 3 weeks. They were dehydrated, embedded in paraffin and serially sectioned at 7 µm.

### Probes and *in situ* hybridization

The mouse *Wnt10a* cDNA was kindly provided by Dr Andrew P. McMahon, Harvard University, Boston, MA. Mouse *Dspp* probes were generated from a 550 bp *Dspp* fragment spanning the region between 656 and 1205 in accession # NM010080. The preparation of *Bmp3* RNA probes has previously been described (Aberg et al., 1997). *In situ* hybridization of paraffin sections using 35S-UTP-labeled riboprobe was performed as described previously (Vainio

et al., 1993). The bright field and dark field images of each section were digitized, and the grains from dark fields were selected, colored red, and added to the bright field pictures in PhotoShop 6 (Åberg et al., 1997). Keratin was used as a marker for epithelial cells and it was detected by immunohistochemistry using polyclonal pan-keratin antibodies (DAKO, A575, Glostrup, Denmark) (Yamashiro et al., 2003).

#### Cell cultures

C3T10T1/2 cell lines, derived from embryonic mouse mesenchyme, were obtained from Riken cell bank (Tsukuba, Japan). These cells were cultured in Dulbecco's modified Eagle's medium (D-MEM, high glucose (4,500 mg/l D-glucose), with L-glutamine, and phenol red) supplemented with 0.1 mM non-essential amino acids (NEAA), 10% fetal bovine serum (FBS), 100 units U/ml penicillin, 100 µg/ml streptomycin, and incubated at 37°C in a 5% carbon dioxide, 95% air, humidified atmosphere. The cells were subcultured every 3–4 days, using 0.05% (w/v) EDTA to detach cells from the culture dish.

#### *Wnt10a* transfection in C3T10T1/2 cells

Mammalian expression vectors encoding mouse *Wnt10* were constructed for transient transfections. Full-length mouse *Wnt10a* cDNA (Wang and Shackleford, 1996), pj32 was kindly provided by Dr. Gregory M. Shackleford, University of Southern California, Los Angeles, CA. *Wnt10a* was transferred from pj32 to the multiple cloning site of pCMV-Script (Stratagene, La Jolla, CA) with the restriction sites *Eco*RI and *Xho*I to generate pCMV-*Wnt10a*. Cells (60%–80% confluence) were transiently transfected with Lipofectamine Plus reagent (Gibco BRL, Gaithersburg, MD) according to the manufacturer's instructions. Briefly, pCMV-*Wnt10a* was mixed with Plus reagent in Opti-MEM I and incubated at room temperature for 15 min. Lipofectamine was mixed with DNA plus reagent and incubated further at room temperature for 15 min. Then the Lipofectamine Plus cDNA complex was added to the cells and incubated at 37°C. The control cells received Lipofectamine Plus alone. After 5 hr of incubation, growth medium containing 20% FBS was added for a final concentration of 10% FBS. The cells were maintained for an additional 12 hr. One day after transfection, cells were plated on Matrigel-coated dishes (Biocoat, Becton Dickinson Labware, Bedford, MA) or conventional culture dishes (Falcon, Becton Dickinson Labware).

#### Western blot analysis of *Wnt10a*

Cell lysate proteins (10 µg) from transfected cells were separated using 7.5% sodium dodecyl sulfate-polyacrylamide gel electrophoresis (SDS-PAGE) and were electrophoretically transferred from gel to polyvinylidene difluoride membranes. To separate non-specific protein binding, the membranes were incubated in 10 mM Tris HCl, pH 7.5, 100 mM NaCl, and 0.1% Tween 20 (TBST) containing 3% blot-qualified bovine serum albumin for 1 hr. The membranes were incubated in TBST containing a 1:1,000 diluted anti-*Wnt10a* antibody (Sigma Genosys Co, Hokkaido, Japan). *Wnt10a* polyclonal rabbit antibody was produced by Sigma Genosys Co based on the *Wnt10a* sequence CRRGDEEAFRR KLHR. *Wnt10a* antibody recognizes a band of approximately 48 kDa that corresponds to the size of *Wnt10a* in *Wnt10a*-transfected cells, while mock-transfected cells gave no signal (Fig. 2B). This signal disappeared after preincubation of the antibody with excess antigenic peptide CRRGDEEAFRRKLHR indicating that the band is specific.

The membrane was washed twice for 15 min each with 0.1% TBST, and incubated for 45 min with the secondary antibody, horseradish peroxidase (HRP)Rabbit-conjugated goat anti-rabbit

(Amersham, Amersham, UK). Bound antibodies were visualized by chemiluminescence using an ECL Western Immunoblotting Kit (Amersham).

#### Reverse-transcriptase polymerase chain reaction (RT-PCR) of *Dspp* and *Wnt10a*

To determine whether *Wnt10a* overexpression in C3H10T1/2 cells induces *Dspp* expression, real-time PCR amplification of *Dspp* was performed. Five, ten and fifteen days after transfection, total RNA was isolated using the RNeasy-kit (Qiagen, Valencia, CA) according to the manufacturer's instructions. First molar tooth germs of the mandible from day 1 postnatal mouse pups were dissected in Dulbecco's PBS under a stereomicroscope. Total RNA was also isolated from tooth germs using the RNeasy-kit (Qiagen). Total RNA (1 µg) was reverse transcribed in 20 µl of transcription buffer [75 mM KCl, 50 mM Tris/HCl pH 8.3, 10 mM dithiothreitol, 3 mM MgCl<sub>2</sub>, 0.5 mM deoxyribonucleotide triphosphate, 1 µg oligo(dT)18-adapter primer] with Superscript II reverse transcriptase (200 U) for 1 hr at 42°C. Presence of *Dspp* and *Wnt10a* mRNA was determined using the LightCycler System and the Faststart DNA Master SYBR Green I kit (both from Roche Diagnostics, Mannheim, Germany). PCRs were performed according to the manufacturer's instructions with 0.5 µm each of the respective forward and reverse primers, 4 mM MgCl<sub>2</sub>, and 1 × Faststart DNA Master SYBR Green I mix in a total volume of 20 µl. Cycling conditions were as follows: 10 min at 94°C, followed by 40 cycles with 15 sec C at 94°C, 10 sec at 64°C and 45 sec at 72°C. Standard GAPDH RT-PCR was used as an internal control for an adequate PCR reaction (472 bp). The following primers were used: 5'-atagcaccaacctgag gct-3' and 5'-ctttgtgcttgggg-3' for *Dspp* gene, 5'-aaccttgccattgt ggaagg-3' and 5'-ggctcctcagtgtgaccaag-3' for *Wnt10a*, 5'-aacttggc attgtggaagg -3' and 5'-ccctgtgtgtagccgtat-3' for GAPDH gene. PCR primer set for *Dspp* was designed for controlling the genomic DNA contamination. Primers that span intron-exon boundaries amplify a product from contaminating DNA that includes the intron, making it larger than the expected cDNA product. The products from the reactions described above were also run on a 1% (w/v) agarose gel, to confirm that all products were of the correct length for the primers used. After amplification, melting curve analysis of the PCR product was used to differentiate between specific and non-specific amplification products. Melting curve was acquired by heating the product at 20°C/sec to 95°C, cooling it at 20°C/sec to 55°C for 30 sec, and slowly heating it at 0.1 µC/sec to 94°C under continuous fluorescence monitoring. Melting curve analysis was accomplished with LightCycler software.

## Results

### Expression of *Wnt10a* and *Dspp* in the developing root

We evaluated the mRNA expression of several *Wnt* genes during root development at postnatal day 14, and found that *Wnt10a* transcripts were specifically present in the dental mesenchymal cells lining the inner dentin surface (Fig. 1A). *Dspp* mRNA was specifically expressed in odontoblasts (Fig. 1B), as shown previously (D'Souza et al., 1997; Bleicher et al., 1999), and both *Wnt10a* and *Dspp* were absent in the dental papilla cells, osteoblasts and cementoblasts.

The epithelial root sheath is a two-cell layer sheet at the apical end of the growing root and it regulates root growth as well as odontoblast differentiation. The root sheath can be visualized by immunohistochemistry

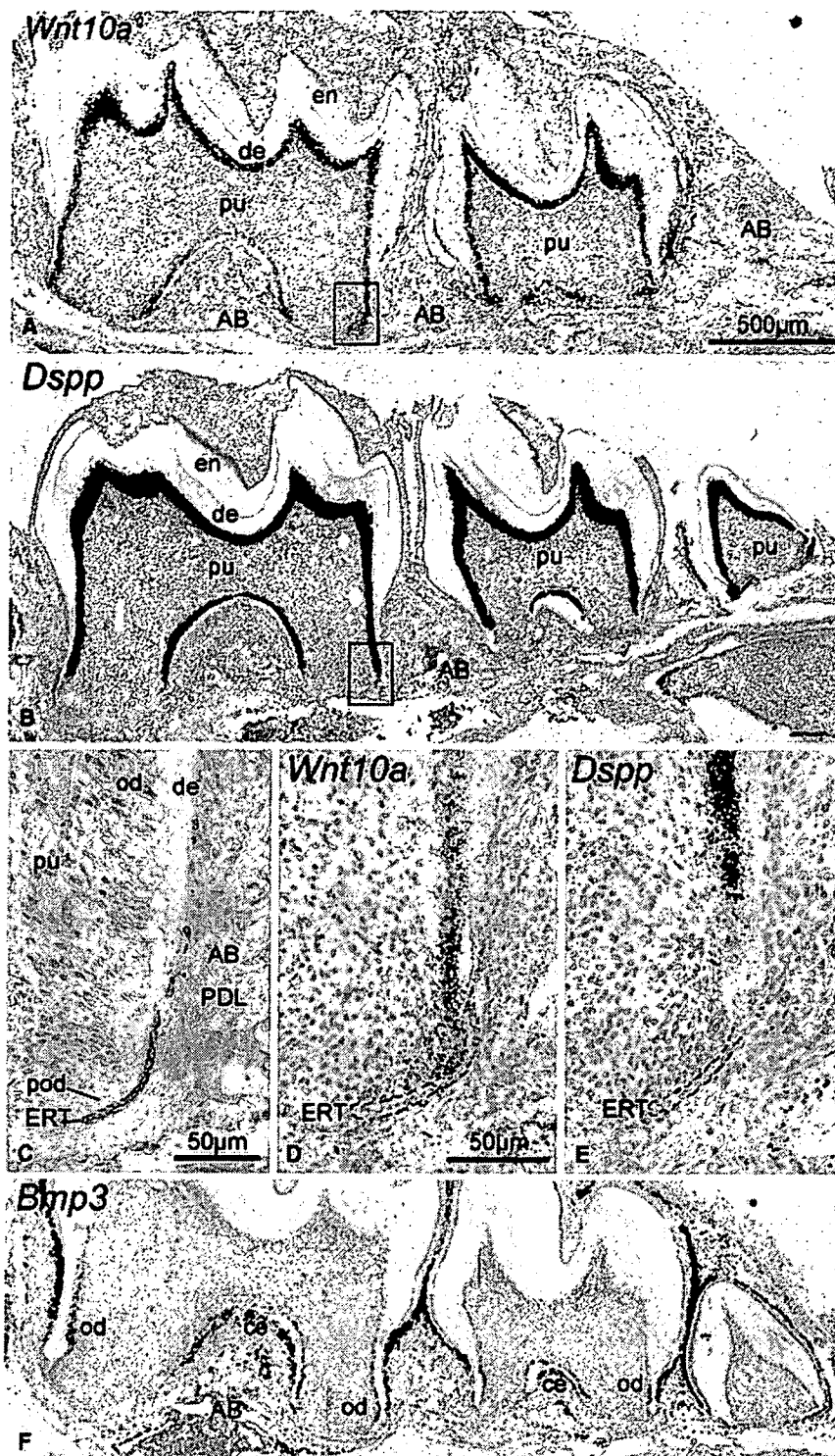


**Fig. 1** *Wnt10a* and *Dspp* mRNA expression in lower jaw sections of a 14-days-old mouse (A, B) *Wnt10a* transcripts were specifically present in the odontoblasts lining the dentin (de) surface but not in the dental papilla cells (pu), or osteoblasts in the alveolar bone (AB). *Dspp* transcripts were also specifically present in odontoblasts. In higher magnification, the epithelial root sheath (ERT) is localized by immunohistochemistry using pan-keratin antibodies. Odontoblasts (od) are columnar cells lining the pulpal surface of dentin (de), and preodontoblasts (pod) are the odontoblast precursors in the apical end of the root. At the apical end of the growing root, *Wnt10a* transcripts were present in the preodontoblasts (pod). (D) The expression was continuous and maintained in differentiating and secretory odontoblasts (od). (E) *Dspp* expression was only detected in polarized odontoblasts (od). en, enamel; PDL, periodontal ligament. (F) Strong *Bmp3* expression was detected in cementoblasts the 1st and 2nd molars, as well as the dental follicle around all three molars. It was also observed in the osteoblasts on the active bone-forming surface.

using pan-keratin antibodies (Fig. 1C). Odontoblasts can be visualized as columnar cells lining the pulpal surface of dentin, and as the gradient of cell differentiation extends towards the root apex, preodontoblasts, i.e. the odontoblast precursors are present next to the

root sheath (Fig. 1C). In higher magnification, *Wnt10a* transcripts were detected in differentiating and secretory odontoblasts and they were also diffusely present in the preodontoblasts underlying the epithelial root sheath (Fig. 1D). Previous reports showed that *Dspp* expres-

sion is initiated with matrix mineralization. *Dspp* was present in polarized odontoblasts but absent in pre-odontoblasts and differentiating odontoblasts indicating that the expression of *Wnt10a* precedes *Dspp* during the differentiation of the odontoblast cell lineage (Fig. 1E). At this stage, osteogenesis and cementogenesis were also active, as shown by intense *Bmp3* signals on the surfaces of bone and cementum (Fig. 1F) (Yamashiro et al., 2002). Hence, *Wnt10a* expression was expressed specifically in secretory odontoblasts

#### *Wnt10a* overexpression induces *Dspp* expression

As *Wnt10a* and *Dspp* transcripts overlapped in the odontoblasts but *Wnt10a* appeared earlier than *Dspp* in the odontoblast cell lineage, we hypothesized that *Dspp* might be induced by *Wnt10a*. To test this possibility, we overexpressed *Wnt10a* in the C310T1/2 cell line and examined its effect on *Dspp* expression. RT-PCR confirmed that C310T1/2 cells and Mock-transfected cells did not express *Wnt10a* mRNA, whereas *Wnt10a* transfected cells at 24 hr post-transfection and the cells derived from P1 tooth germs showed 340-bp bands of *Wnt10a* (Fig. 2A).

Induction of *Dspp* expression was detected in the *Wnt10a* transfected cells by real-time PCR ten days after transfection, but not after five or fifteen days. C3H10T1/2 cells did not show *Dspp* expression (Figs. 3A,3B). Gel electrophoresis of RT-PCR products (40 cycles) demonstrate a single band of 550 bp, corresponding to the *Dspp* transcript in cDNA derived from total RNA obtained from C310T1/2 cells transfected with pCMV-Wnt10a and cultured on Matrigel (*Wnt10a* Mg(+)), and positive control (tooth germ; Fig. 3B), indicating that *Dspp* induction was seen only when the cells were cultured on Matrigel coated dishes. Matrigel is an extract of basement membrane proteins (Kleinman et al., 1982 #16), and *Wnt10a* transfected cells cultured on conventional collagen coated dishes did not express *Dspp*. Mock transfected cells cultured on Matrigel dishes did not show *Dspp* expression (Figs. 3A,3B), indicating that Matrigel itself did not induce *Dspp*. These results indicated that *Wnt10* can induce *Dspp* expression and that the specific basement membrane matrix was essential for this induction.

We confirmed the specificity of the amplified products and PCR products were not detected in Mock-transfected cells. The integrity of the RT-PCR products was confirmed by melting curve analysis (Fig. 3C). Melting curve analysis showed that the  $T_m$  of the *Dspp* templates was 88.5°C and occurred as a single amplicon peak for both *Wnt10a* transfected cells and control samples, reflecting the specificity of the PCR-products (Fig. 3C). The non-specific products, such as primer dimers, sometimes appeared, however, they melt below 80°C and were differentiated from the specific products by the melting curve analysis. These results were also

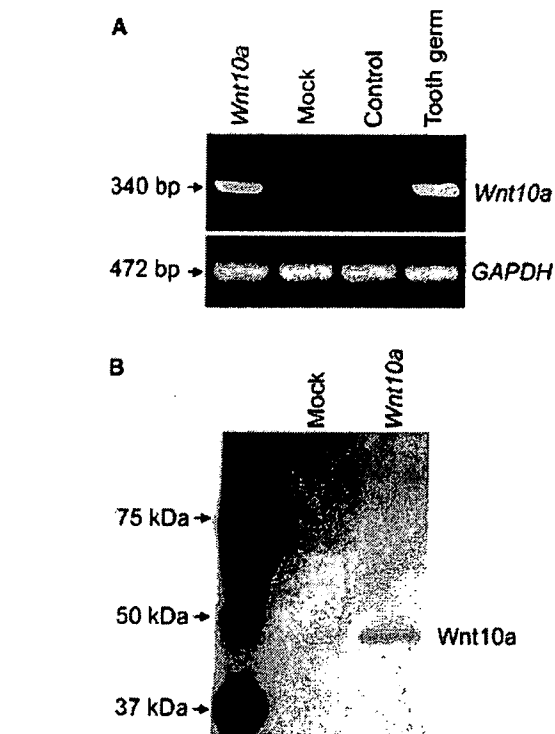


Fig. 2 C310T1/2 cells were transiently transfected with expression vectors encoding *Wnt10a*. (A) Expression of *Wnt10a* mRNA in C310T1/2 cells. After 24 hr transient transfection, total mRNA was extracted and submitted to reverse-transcriptase polymerase chain reaction (RT-PCR) using oligonucleotide primers specific of *Wnt10a* and *GAPDH*. Cells were transfected with pCMV-Wnt10a (*Wnt10a*) or its vehicle pCMV (Mock). Total RNA was also isolated from tooth germs and used as a positive control (tooth germ, 30 cycles). Negative control (control, 30 cycles) was performed in the absence of oligonucleotides. RT-PCR confirmed transfection efficiency using pCMV-WNT10a (*Wnt10a*, 30 cycles). (B) Expression of *Wnt10a* protein in C310T1/2 cells. Overexpression of *Wnt10a* protein was also confirmed by Western blot analysis 48 hr after transfection. Cells were lysed in sodium dodecyl sulfate-polyacrylamide gel electrophoresis (SDS-PAGE) loading buffer after transfection and analyzed by Western blot with specific antibodies to *Wnt10a*. pCMV-Wnt10-transfected (*Wnt10a*) cells showed *Wnt10a* protein expression. This protein expression was not observed in control cells transfected with vehicle pCMV (Mock). A molecular weight marker was run in parallel in the first lane.

confirmed by gel electrophoresis. Transfection and PCR were repeated three times.

#### Expression of *Wnt10a* during tooth development

At E14, the cap stage of tooth development, *Wnt10a* transcripts were intensely expressed in the enamel knot, as shown previously (Dassule and McMahon, 1998). No *Wnt10a* expression was detected in the dental mesenchyme (Fig. 4A). At E16, early bell stage, the primary enamel knot had disappeared, and *Wnt10a* was detected in secondary enamel knots. In addition, the mesenchymal cells directly underlying the enamel knots expressed *Wnt10a* (Fig. 4B). Subsequently at E18 transcripts were



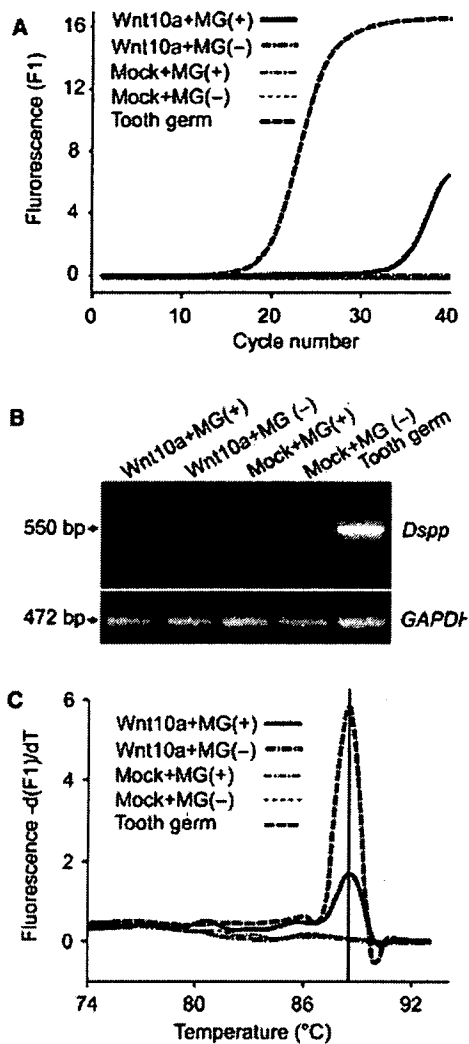


**Fig. 3** Wnt10a transient transfection in C310T1/2 cells induced dentin sialophosphoprotein (Dsp) gene expression. (A) C310T1/2 cells were transiently transfected with pCMV-Wnt10a (Wnt10a) or its vehicle pCMV (Mock). Transfected cells were harvested 10 day post-transfection on Matrigel (Mg (+)) or collagen coated dishes (Mg (-)). Total mRNA extracted from the transfected cells was reverse transcribed and submitted to real-time polymerase chain reaction (PCR) using oligonucleotide primers specific of Dsp. Total RNA was also isolated from tooth germs and used as a positive control (Tooth germ). The x-axis denotes the cycle number of a quantitative PCR assay, and the y axis denotes the fluorescence intensity (F1) over the background. Amplification of Dsp was observed in C310T1/2 cells transfected with pCMV-Wnt10a and cultured on Matrigel (Wnt10a+Mg (+)), and positive control (tooth germ). (B) Forced-expression of Wnt10a induced Dsp expression when the transfected cells were cultured on Matrigel dishes (Wnt10a+Mg (+), 40 cycles). Wnt10a transfected cells cultured on normal culture dishes (Wnt10a+Mg (-), 40 cycles) and Mock transfected cells cultured on Matrigel dishes (Mock+Mg (+), 40 cycles) or normal culture dishes (Mock+Mg (-), 40 cycles) did not show Dsp expression. Positive control (Tooth germ) showed intense Dsp expression. (C) PCR products were subjected to melting peak analyses to determine the specificity of the products. Dsp sample showed a single product with  $T_m$  values of 88.5°C.

accumulated in the single cell layer of differentiating odontoblasts, which were aligned under the basement membrane (Fig. 4C). At E18, the differentiating odontoblasts became polarized and odontoblast differentiation initiated from the tips of the future cusps where the enamel knots are located (Fig. 5A). As the differentiation of preodontoblasts proceeded from the cusp tips in cervical direction along the cusp slopes *Wnt10a* expression was intimately linked with this gradient of differentiation. (Fig. 5B), and was highest in the cusp regions (Fig. 5C). *Dsp* expression was not yet expressed in the odontoblast lineage at this stage (Bleicher et al., 1999). In the early osteogenesis, *Wnt10a* was detected in the future bone regions at E13 and E14 (data not shown). This expression was down-regulated significantly at E16 and the expression could not be detected at P14 (Fig. 1A).

## Discussion

The expression pattern of *Wnt10a* is associated with odontoblast differentiation

Our *in situ* hybridization analysis revealed that the expression of *Wnt10a* mRNA was associated with dentinogenesis. We found that *Wnt10a* expression was intense in the odontoblast cell layer and that it was maintained specifically in secretory odontoblasts where it was coexpressed with *Dsp*. In root development stage, mineralized matrix is also actively formed on the surface of bone and cementum, and the distribution of *Bmp3* expression indicated the regions of active osteogenesis and cementogenesis at the root surface and the surrounding alveolar bone surface. The comparison of *Wnt10a* and *Bmp3* distribution revealed that *Wnt10a* expression was specifically involved in odontogenesis, but not in osteogenesis or cementogenesis.

At the tip of the growing root, Hertwig's epithelial root sheath proliferates and directs root morphogenesis. The pulpal mesenchyme provides precursors for odontoblasts, and the subpopulation of pulp cells that contact the epithelial root sheath differentiate into preodontoblasts. As odontoblast differentiation is characterized by cytological polarization and they are lining in one cell layer they can be clearly distinguished from the surrounding pulpal cells. *In situ* hybridization analysis demonstrated that *Wnt10a* was not expressed in the pulpal mesenchyme, indicating that Wnt10a is induced when the precursor cells start to differentiate into odontoblasts.

Wnt10a regulates the expression of *Dsp*

*Dsp* and *Wnt10a* were colocalized in the differentiated odontoblasts. However, at the tip of the growing root,

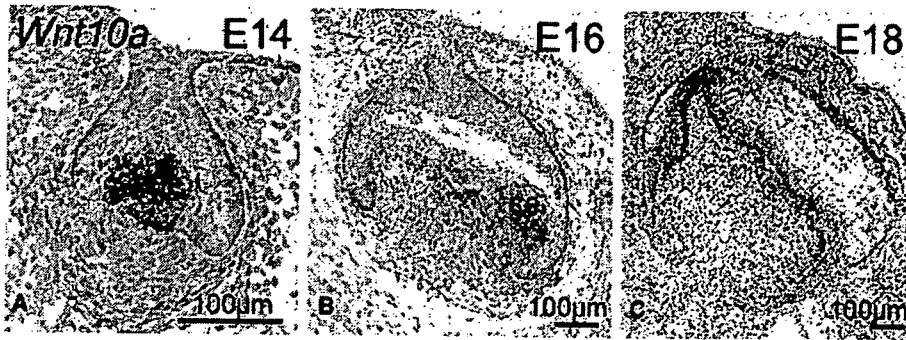


Fig. 4 At E14 (cap stage) *Wnt10a* transcripts were present in the primary enamel knot (pe), as shown previously. No expression was detected in the dental mesenchyme (A). At E16 (early bell stage) *Wnt10a* was detected in secondary enamel knots (se). In addition gene expression had shifted to the underlying mesenchymal cells (B). At E18 transcripts were accumulated in the single cell layer of differentiating odontoblasts (C).

*Wnt10a* expression was present in preodontoblasts beneath the epithelial sheath, but *Dspp* expression was absent indicating that *Wnt10a* expression appeared earlier than *Dspp* expression. Similarly, in early tooth development *Wnt10a* expression was first initiated in the odontogenic lineage cells at E14 whereas *Dspp* appeared in odontoblasts at E17 (Yamazaki et al., 1999). This temporo-spatial distribution pattern was in line with the possibility of an inductive role of *Wnt10a* on *Dspp* expression and we confirmed by transient overexpression of *Wnt10a* in C310T1/2 cells that *Dspp* was downstream of *Wnt10a*. The C310T1/2 cell line is derived from embryonic mesodermal cells, and can differentiate into distinctly different cell lineages, myoblasts, adipocytes, chondrocytes and osteoblasts under the influence of certain inducers (Taylor and Jones, 1979; Katagiri et al., 1990; Asahina et al., 1996). As C310T1/2 cells did not constitutively express either *Wnt10a* or *Dspp* mRNA, our data indicated that *Dspp* was induced by *Wnt10a* in C310T1/2 cells and that it may be a direct downstream target of *Wnt10a* (Fig. 6).

The extracellular mineralizing matrices of dentin and bone share many similarities, and it is likely that regulation of osteoblast and odontoblast differentiation may involve same signaling molecules (Thesleff et al., 2001). To our knowledge, *Wnt10a* is the first signal molecule that has specifically associated with odontoblast differ-

entiation. Various Wnt genes, such as *Wnt1*, *Wnt4*, *Wnt5a*, *Wnt9a/14* and *Wnt7b*, are expressed in either osteoblast precursors or adjacent tissues during embryonic development, and *Wnt3a* and *Wnt10b* are expressed in bone marrow (Hartmann, 2006). In our study, we also demonstrated that *Wnt10a* was expressed in the future bone regions, but its expression was not maintained in the postnatal bone. Among these Wnt molecules, *Wnt10b* mutants display a postnatal decrease in bone mass and serum osteocalcin level, indicating that *Wnt10b* is an endogenous regulator of bone formation (Bennett et al., 2005). *Wnt10b* is homologous to *Wnt10a*, and *WNT6* and *WNT10a* genes are clustered in tail-to-head manner. Like *Wnt10a*, both *Wnt10b* and *Wnt6* are expressed in the enamel knot and the dental epithelium in early tooth development (Dassule and McMahon, 1998; Sarkar and Sharpe, 1999). However, during later tooth development, *Wnt6* or *Wnt10b* transcripts were not detected in the odontoblast cell lineage by *in situ* hybridization (data not shown).

Cell to matrix interactions are required for the induction of *Dspp* expression by *Wnt10a*

Studies in the 1970's and 1980's showed that odontoblast differentiation depends on contacts between the

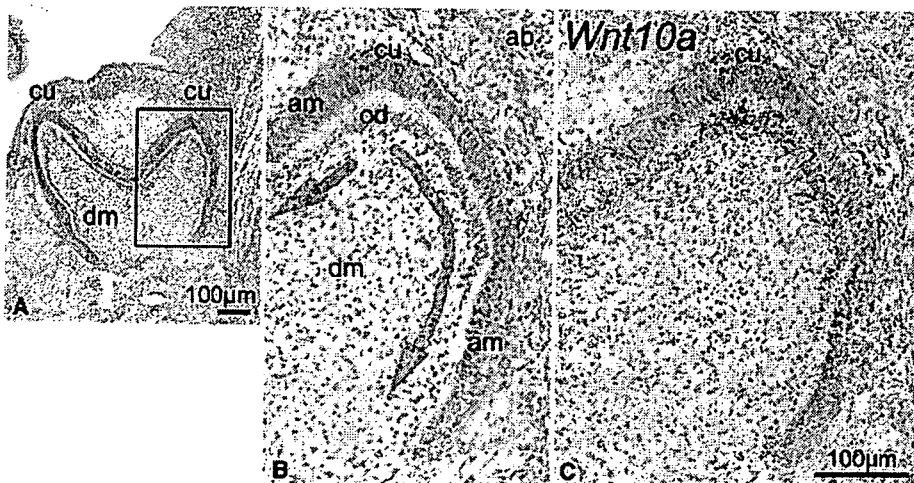
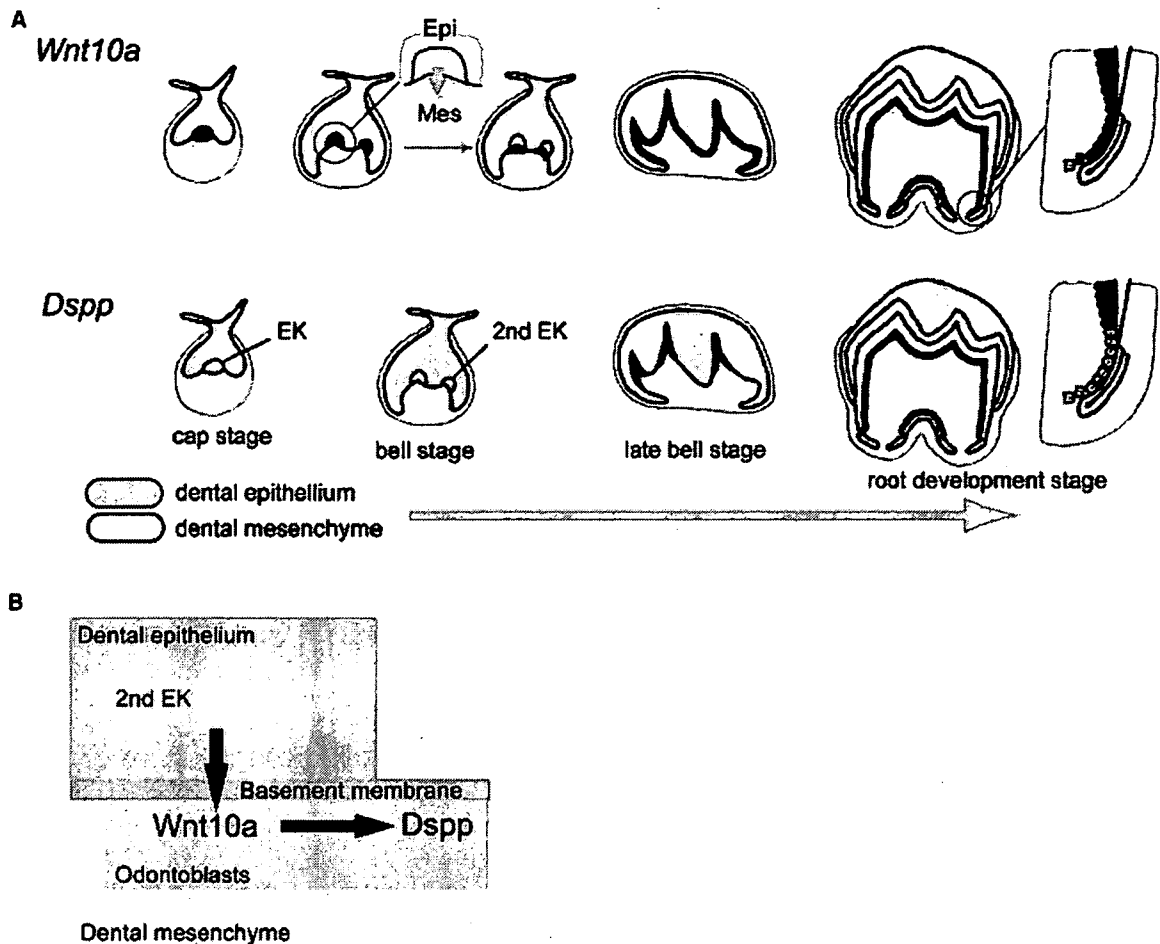


Fig. 5 Coronal sections of E18 molar (late bell stage) (A). (B) Higher magnification of the labial half of 1st molar (inset in panel A). Odontoblast differentiation has initiated beneath the forming cusp (cu) and the cells have polarized. (C). *Wnt10a* expression is associated with the gradient of odontoblast cytodifferentiation, and is highest in the cusp regions (cu).



**Fig. 6 (A)** Summary of the expression of *Wnt10a* and *Dspp* during tooth development. *Wnt10a* is expressed in the enamel knot (EK) at the cap stage. At the bell stage, *Wnt10a* is expressed in the secondary enamel knot (2nd EK), and the expression has shifted to the underlying mesenchyme. In the late bell stages, *Wnt10a* expression is continuous in the preodontoblasts and odontoblasts. *Dspp* is expressed in the odontoblasts in the cusp regions. During root development, both *Wnt10a* and *Dspp* expression domains overlap in the odontoblasts. However, *Wnt10a* expression appeared earlier in

the differentiating preodontoblasts underlying the epithelial root sheath. **(B)** Schematic diagram illustrating induction of *Dspp* expression by *Wnt10a* signals in the odontoblast cell lineage. *Wnt10a* appears in the mesenchymal cells beneath the secondary enamel knots. *Wnt10a* induces *Dspp* expression in the odontoblasts, and cell to matrix interactions are required for the induction of *Dspp* expression by *Wnt10a*. Hence, *Wnt10a* links tooth morphogenesis and odontoblast differentiation.

mesenchymal cells and the basement membrane underlying the enamel epithelium (Thesleff and Hurmerinta, 1981). Many extracellular matrix molecules were implicated in the cell–matrix interactions including fibronectin and other glycoproteins as well as proteoglycans. It was also suggested that growth factors and other diffusible molecules may have been trapped in the basement membrane, and involved in communication between cells. Interestingly, *Dspp* was induced only when the *Wnt10a*-transfected cells were cultured on Matrigel, which is an extract of basement membrane proteins (Kleinman et al., 1982), supporting the idea that cell to matrix association plays some role in odontoblast differentiation. As Mock-transfected cell did not show *Dspp* expression on Matrigel, Matrigel itself can-

not induce odontogenesis. Among various molecules in the basement membrane, laminin alpha2 is subunit of laminin-2. Laminin- $\alpha$ 2 deficiency resulted in a dramatic decrease in *Dspp* expression in odontoblasts (Yuasa et al., 2004), which is in agreement with our data and also supports the idea that cell–matrix interaction is essential for *Dspp* expression.

Heparan sulfate proteoglycans are major components of the extracellular matrix and regulate the transmission of developmental signals (Hacker et al., 2005). They also modulate the Wnt pathway (Haerry et al., 1997). In tooth development, odontoblast differentiation was inhibited *in vitro* by tunicamycin, which inhibited protein glycosylation and the accumulation of proteoglycans and glycoproteins in the basement mem-

brane of the developing tooth (Thesleff and Pratt, 1980). In tooth development also the cell surface proteoglycan syndecan-1 is involved in epithelial–mesenchymal interactions (Vainio et al., 1989; Thesleff et al., 1991), and syndecan-3 has been detected in the odontoblast layer underlying the inner enamel epithelium (Hikake et al., 2003). Heparin-sulfated forms of proteoglycans (HSPG) are long proteins with branched sugar side chains that are expressed on the cell surface, and can form complexes with a variety of signaling molecules, including Wnts and fibroblast growth factors (Nybakken and Perrimon, 2002). Hence it is possible that *Wnt10a* can be captured in the basement membrane extracellular matrix molecules to control differentiation of the pulp cells into odontoblasts. In addition, spatial distribution patterns of *Wnt10a* mRNA expression, together with previous findings, might provide an insight into a possible association between Wnt signaling and heparan sulfate proteoglycan in dentinogenesis. With tooth development, the basement membrane degrades and odontoblasts come into contact with the predentin surface. As predentin also contains various extracellular matrix molecules, such as proteoglycan and fibronectin (Linde and Goldberg, 1993), the cell–matrix interaction between odontoblasts and predentin might thus be explained the continuous expression of *Wnt10a* and *Dspp* in odontoblasts after the basement membrane has disappeared.

In our study, transfected cells were cultured on Matrigel in the medium supplemented with serum. Although both serum and Matrigel contain many growth factors and proteins these did not induce odontoblast differentiation as shown by the lack of *Dspp* expression in Mock transfected cells. Our real-time PCR data demonstrated that the *Dspp* induction by forced over-expression of *Wnt10a* was specific.

Odontoblast differentiation is regulated by reciprocal epithelial mesenchymal interactions. In addition, *Dspp* is expressed in a time- and site-specific manner and *Dspp*-expressing odontoblasts lie in one cell layer. These findings suggest that *Dspp* expression could be regulated by several inhibitory and stimulatory factors in a coordinated manner. Our real-time PCR data showed that *Dspp* induction in *Wnt10a* transfected non-odontogenic cells was much less than the *Dspp* expression in intact odontoblasts. These data suggested that *Wnt10a* thus plays an important role in *Dspp* induction, however, further interaction with other putative molecules might be necessary to express a sufficient amount of *Dspp* during odontoblast differentiation.

#### *Wnt10a* and tooth morphogenesis

In the early tooth, *Wnt10a* is expressed in the enamel knot (Dassule and McMahon, 1998), which has a central function in the control of growth and patterning of

the tooth crown (Jernvall and Thesleff, 2000; Miletich and Sharpe, 2003). Our *in situ* hybridization analysis showed that *Wnt10a* expression was reiterated in the secondary enamel knots which express most of the same signal molecules as the primary enamel knots and initiate cusp formation (Fig. 6A) (Vaahtokari et al., 1996). Interestingly, we found that *Wnt10a* expression shifted from the secondary enamel knots to the underlying mesenchyme. It could be that mesenchymal *Wnt10a* expression was induced by signaling molecules of the secondary enamel knots, perhaps by *Wnt10a* itself. The continuous *Wnt10a* mRNA distribution pattern in the odontoblasts suggested autocrine regulation of *Wnt10a* expression in the mesenchymal cells after the initial induction of *Wnt10a* by the epithelium.

Our study has provided new insight into the molecular mechanisms that spatially and temporally control the initiation of odontoblast differentiation. The terminal differentiation of odontoblasts is initiated at the tip of each cusp, indicating that the cell fate decision and morphogenesis is tightly linked (Fig. 6B). As both the initiation of odontoblast differentiation and the initiation of cusps coincide temporally and spatially with the secondary enamel knots, and as both processes are induced by epithelial signals (Jernvall et al., 1994; Jernvall and Thesleff, 2000), it is conceivable that some signals could regulate both cell differentiation as cusp morphogenesis. Our observations indicated that the expression of *Wnt10a* was intimately linked with the secondary enamel knots and the gradient of cytodifferentiation-propagating apically from each cusp tip. Our data clearly demonstrated that *Wnt10a*-shifting from the epithelial signaling center to the underlying mesenchyme temporally and spatially corresponds to the initiation of odontoblast differentiation. In addition, functional network of *Wnt10a* and the cell to matrix interactions may trigger and regulate tooth specific *Dspp* expression. Putative matrix molecules may provide the cues for polarization of the cells, which may be necessary also for the transmission of the *Wnt10a* signal from the epithelium to the preodontoblast.

In summary, we found that *Wnt10a* was specifically expressed in the odontoblast cell lineage in mouse molars with striking colocalization with *Dspp* mRNA expression in the fully differentiated secretory odontoblasts. *Dspp* is a key molecule for dentin mineralization, and we showed that the forced expression of *Wnt10a* induced *Dspp* mRNA in pluripotent fibroblast cells, indicating that *Wnt10a* is possibly involved in dentine mineralization as an upstream regulator of *Dspp*. However, our observation that *Dspp* was induced only when the transfected cells were cultured on Matrigel suggests that cell to matrix interactions have crucial roles in dentinogenesis in conjunction with *Wnt10a*. This supports earlier proposals that odontoblast differentiation requires interactions between the mesenchymal cells and the extracellular matrix. We also found

that *Wnt10a* was expressed in the epithelial secondary enamel knots, and that this expression shifted to the underlying mesenchymal cells. The timing and location of this shift corresponds to the initiation of the polarization of preodontoblasts. Taken together, our findings indicate that *Wnt10a* and cell to matrix interactions play an important role for odontoblast differentiation and that *Wnt10a* links tooth morphogenesis and the differentiation of odontoblasts.

**Acknowledgments** We thank Merja Mäkinen and Riikka Santalahti for their excellent technical assistance. This study was supported by Grants-in-Aid for Scientific Research from the Japan Society for the Promotion of Science, the Academy of Finland, and the Sigrid Juselius Foundation.

## References

- Åberg, T., Wozney, J. and Thesleff, I. (1997) Expression patterns of bone morphogenetic proteins (Bmps) in the developing mouse tooth suggest roles in morphogenesis and cell differentiation. *Dev Dyn* 210:383–396.
- Asahina, I., Sampath, T.K. and Hauschka, P.V. (1996) Human osteogenic protein-1 induces chondroblastic, osteoblastic, and/or adipocytic differentiation of clonal murine target cells. *Exp Cell Res* 222:38–47.
- Bennett, C.N., Longo, K.A., Wright, W.S., Suva, L.J., Lane, T.F., Hankenson, K.D. and MacDougall, O.A. (2005) Regulation of osteoblastogenesis and bone mass by *Wnt10b*. *Proc Natl Acad Sci USA* 102:3324–3329.
- Bleicher, F., Couble, M.L., Farges, J.C., Couble, P. and Magloire, H. (1999) Sequential expression of matrix protein genes in developing rat teeth. *Matrix Biol* 18:133–143.
- Cadigan, K.M. and Nusse, R. (1997) Wnt signaling: a common theme in animal development. *Genes Dev* 11:3286–3305.
- Dassule, H.R. and McMahon, A.P. (1998) Analysis of epithelial-mesenchymal interactions in the initial morphogenesis of the mammalian tooth. *Dev Biol* 202:215–227.
- D'Souza, R.N., Cavender, A., Sunavala, G., Alvarez, J., Ohshima, T., Kulkarni, A.B. and MacDougall, M. (1997) Gene expression patterns of murine dentin matrix protein 1 (*Dmp1*) and dentin sialophosphoprotein (*DSPP*) suggest distinct developmental functions in vivo. *J Bone Miner Res* 12:2040–2049.
- Feng, J.Q., Luan, X., Wallace, J., Jing, D., Ohshima, T., Kulkarni, A.B., D'Souza, R.N., Kozak, C.A. and MacDougall, M. (1998) Genomic organization, chromosomal mapping, and promoter analysis of the mouse dentin sialophosphoprotein (*Dspp*) gene, which codes for both dentin sialoprotein and dentin phosphoprotein. *J Biol Chem* 273:9457–9464.
- Hacker, U., Nybakken, K. and Perrimon, N. (2005) Heparan sulphate proteoglycans: the sweet side of development. *Nat Rev Mol Cell Biol* 6:530–541.
- Haerry, T.E., Heslip, T.R., Marsh, J.L. and O'Connor, M.B. (1997) Defects in glucuronate biosynthesis disrupt Wingless signaling in *Drosophila*. *Development* 124:3055–3064.
- Hartmann, C. (2006) A Wnt canon orchestrating osteoblastogenesis. *Trends Cell Biol* 16:151–158.
- Hikake, T., Mori, T., Iseki, K., Hagino, S., Zhang, Y., Takagi, H., Yokoya, S. and Wanaka, A. (2003) Comparison of expression patterns between CREB family transcription factor OASIS and proteoglycan core protein genes during murine tooth development. *Anat Embryol (Berlin)* 206:373–380.
- James, M.J., Jarvinen, E. and Thesleff, I. (2004) Bonol: a gene associated with regions of deposition of bone and dentine. *Gene Expr Patterns* 4:595–599.
- Jernvall, J., Kettunen, P., Karavanova, I., Martin, L.B. and Thesleff, I. (1994) Evidence for the role of the enamel knot as a control center in mammalian tooth cusp formation: non-dividing cells express growth stimulating *Fgf-4* gene. *Int J Dev Biol* 38:463–469.
- Jernvall, J. and Thesleff, I. (2000) Reiterative signaling and patterning during mammalian tooth morphogenesis. *Mech Dev* 92:19–29.
- Katagiri, T., Yamaguchi, A., Ikeda, T., Yoshiki, S., Wozney, J.M., Rosen, V., Wang, E.A., Tanaka, H., Omura, S. and Suda, T. (1990) The non-osteogenic mouse pluripotent cell line, C3H10T1/2, is induced to differentiate into osteoblastic cells by recombinant human bone morphogenetic protein-2. *Biochem Biophys Res Commun* 172:295–299.
- Kleinman, H.K., McGarvey, M.L., Liotta, L.A., Robey, P.G., Tryggvason, K. and Martin, G.R. (1982) Isolation and characterization of type IV procollagen, laminin, and heparan sulfate proteoglycan from the EHS sarcoma. *Biochemistry* 21:6188–6193.
- Kollar, E.J. (1985) Tissue interactions in development of teeth and related ectodermal derivatives. *Dev Biol (NewYork)* 4:297–313.
- Kratochwil, K., Galceran, J., Tontsch, S., Roth, W. and Grosschedl, R. (2002) FGF4, a direct target of LEF1 and Wnt signaling, can rescue the arrest of tooth organogenesis in *Lef1* (–/–) mice. *Genes Dev* 16:3173–3185.
- Lesot, H., Lisi, S., Peterkova, R., Peterka, M., Mitolo, V. and Ruch, J.V. (2001) Epigenetic signals during odontoblast differentiation. *Adv Dent Res* 15:8–13.
- Linde, A. and Goldberg, M. (1993) Dentinogenesis. *Crit Rev Oral Biol Med* 4:679–728.
- Miletich, I. and Sharpe, P.T. (2003) Normal and abnormal dental development. *Hum Mol Genet* 12(Spec No 1):R69–R73.
- Nakashima, M., Nagasawa, H., Yamada, Y. and Reddi, A.H. (1994) Regulatory role of transforming growth factor-beta, bone morphogenetic protein-2, and protein-4 on gene expression of extracellular matrix proteins and differentiation of dental pulp cells. *Dev Biol* 162:18–28.
- Nusse, R. (2003) Wnts and Hedgehogs: lipid-modified proteins and similarities in signaling mechanisms at the cell surface. *Development* 130:5297–5305.
- Nybakken, K. and Perrimon, N. (2002) Heparan sulfate proteoglycan modulation of developmental signaling in *Drosophila*. *Biochim Biophys Acta* 1573:280–291.
- Qin, C., Brunn, J.C., Cadena, E., Ridall, A., Tsujigiwa, H., Nagatsuka, H., Nagai, N. and Butler, W.T. (2002) The expression of dentin sialophosphoprotein gene in bone. *J Dent Res* 81:392–394.
- Rajpar, M.H., Koch, M.J., Davies, R.M., Mellody, K.T., Kielty, C.M. and Dixon, M.J. (2002) Mutation of the signal peptide region of the bicistronic gene *DSPP* affects translocation to the endoplasmic reticulum and results in defective dentine biomineralization. *Hum Mol Genet* 11:2559–2565.
- Ruch, J.V., Lesot, H., Karcher-Djuricic, V., Meyer, J.M. and Olive, M. (1982) Facts and hypotheses concerning the control of odontoblast differentiation. *Differentiation* 21:7–12.
- Sarkar, L. and Sharpe, P.T. (1999) Expression of Wnt signalling pathway genes during tooth development. *Mech Dev* 85:197–200.
- Shiba, H., Fujita, T., Doi, N., Nakamura, S., Nakanishi, K., Takemoto, T., Hino, T., Noshiro, M., Kawamoto, T., Kurihara, H. and Kato, Y. (1998) Differential effects of various growth factors and cytokines on the syntheses of DNA, type I collagen, laminin, fibronectin, osteonectin/secreted protein, acidic and rich in cysteine (SPARC), and alkaline phosphatase by human pulp cells in culture. *J Cell Physiol* 174:194–205.
- Shields, E.D., Bixler, D. and el-Kafrawy, A.M. (1973) A proposed classification for heritable human dentine defects with a description of a new entity. *Arch Oral Biol* 18:543–553.
- Sreenath, T., Thyagarajan, T., Hall, B., Longenecker, G., D'Souza, R., Hong, S., Wright, J.T., MacDougall, M., Sauk, J. and